Universal Time-Entanglement Trade-Off in Open Quantum Systems

Andrew Pocklington[1,2,*] and Aashish A. Clerk[2]

[1]*Department of Physics, University of Chicago, 5640 South Ellis Avenue, Chicago, Illinois 60637, USA*
[2]*Pritzker School of Molecular Engineering, University of Chicago, Chicago, Illinois 60637, USA*

We demonstrate a surprising connection between pure steady-state entanglement and relaxation time scales in an extremely broad class of Markovian open systems, where two (possibly many-body) systems, *A* and *B*, interact locally with a common dissipative environment. This setup also encompasses a broad class of adaptive quantum dynamics based on continuous measurement and feedback. As steady-state entanglement increases, there is generically an emergent strong symmetry that leads to a dynamical slow-down. Using this, we can prove rigorous bounds on relaxation times set by steady-state entanglement. We also find that this time must necessarily diverge for maximal entanglement. To test our bound, we consider the dynamics of a random ensemble of local Lindbladians that support pure steady states, finding that the bound does an excellent job of predicting how the dissipative gap varies with the amount of entanglement. Our work provides general insights into how dynamics and entanglement are connected in open systems and has specific relevance to quantum reservoir engineering.

I. INTRODUCTION

An exciting and powerful recent direction in quantum many-body physics is the realization that dynamical properties can be directly related to ground-state entanglement features. For example, pioneering work by Hastings has shown that the ground states of finite-range gapped one-dimensional (1D) Hamiltonians obey an entanglement area law [1]. Under certain conditions, this result can be extended to longer-range interactions [2,3] and higher dimensions [4–10], (for a review, see Ref. [11]). By understanding aspects of the energy spectrum of a many-body-system, one can obtain extremely nontrivial information about the structure of entanglement in its ground state.

In this work, we show that nontrivial connections between steady-state bipartite entanglement and dynamical properties can also be established in open quantum systems supporting pure steady states. Focusing on many-body Markovian dissipative systems [described by a Gorini-Kossakowski-Sudarshan-Lindblad (GKSL)–Lindblad master equation [12,13]] satisfying only weak locality constraints, we show that systems with pure *maximally* entangled steady states necessarily exhibit dynamical

isolation: there is an emergent strong symmetry that makes it impossible to prepare the entangled steady state in finite time. This phenomenon implies a vanishing of the dissipative gap.

Further, for systems with nonmaximal steady-state entanglement, we prove an inequality that sets a lower bound on the preparation time of the steady state. This bound shows that the time required to reach the steady state grows exponentially in the Renyi-2 entanglement entropy of the steady state. The general setup that we consider [see Fig. 1] also directly constrains a broad class of measurement and feedback protocols, the unconditional dynamics of which result in steady-state entanglement. We thus establish a fundamental trade-off between steady-state entanglement generation and relaxation times for an extremely wide class of nonunitary dynamics. Note that previous work on open systems has established relations between steady-state correlations and the dissipative gap [14–16]; however, unlike our work, these results only apply in the thermodynamic limit and do not connect bipartite entanglement and relaxation times.

Our result has strong implications for the general techniques of reservoir engineering and autonomous feedback [17,18]. Such approaches are ubiquitous in quantum information processing and involve employing tailored dissipative processes to prepare and stabilize useful quantum steady states. Perhaps the most common kind of target states here are those with long-range entanglement (see, e.g., Refs. [19–37]). While extremely powerful, reservoir engineering is only practically effective if the relevant

---

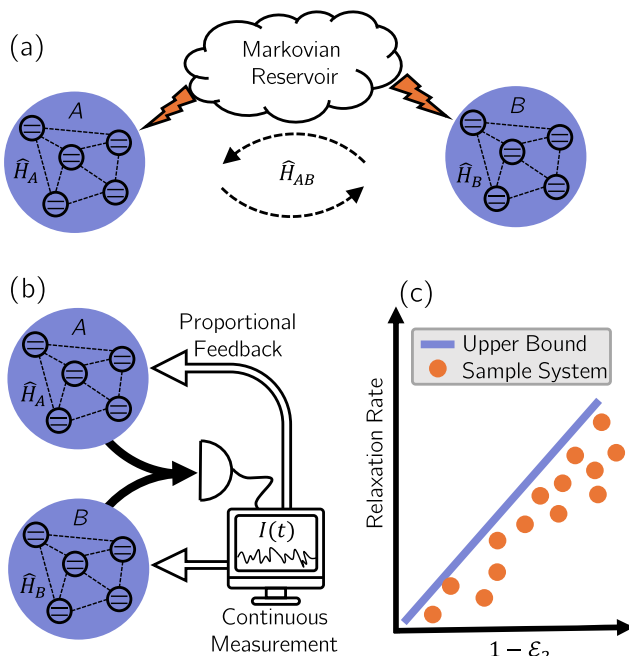*Contact author: abpocklington@uchicago.edu

FIG. 1. (a) A schematic showing two arbitrary systems, A and B, interacting dissipatively via local couplings to a common Markovian reservoir, along with arbitrary intrasystem ($\hat{H}_A$, $\hat{H}_B$) as well as intersystem ($\hat{H}_{AB}$) Hamiltonian interactions. We focus on cases in which the dynamics lead to pure steady states with finite entanglement. (b) The above dynamics are equivalent to a generic adaptive measurement setup: a continuous collective measurement is made of A and B and the result $I(t)$ is used to drive both systems. (c) Our key result is that the relaxation rate to the steady state is bounded above by $1 - \mathcal{E}_2$, where $\mathcal{E}_2$ is the scaled steady-state entanglement [cf. Eq. (17)]. $(1 - \mathcal{E}_2)$ is zero for maximally entangled states, indicating that the dissipative gap must close in such cases.

relaxation rates are sufficiently fast (otherwise, intrinsic uncontrolled dissipative processes will corrupt the eventual steady state). Our fundamental entanglement-time trade-off directly applies to this setting. Previous work has phenomenologically seen evidence of such a trade-off in a variety of different schemes; i.e., the preparation time would diverge as the steady state was engineered to have maximal entanglement [29,30,36]. In the simplest specific case of two qubits, this trade-off could be connected to an effective conservation of angular momentum that emerged in the maximum-entanglement limit [30]. Our results establish the origin of this trade-off in the most general many-body setting and have far-reaching implications on the design of optimal entanglement-stabilization protocols. Note that for two qubits, studies have shown how to evade dynamical slow-down by using additional energy levels [26,30]. Such an approach effectively changes the local Hilbert-space dimensions (and thus the maximum possible amount of entanglement) and thus a version of our bound still applies.

One might worry that while our work sets an upper bound on time scales for dissipative remote entanglement stabilization, this bound might be extremely loose and have little relevance to typical systems. To address this, we first solve a seemingly complex inverse problem: given a specific many-body entangled pure state of interest, how do we reverse engineer a local dissipative process that will stabilize it? We provide a very general construction that solves this challenge and use it to construct a set of local random Lindbladians that all stabilize a given target state. Using this ensemble of random Lindbladians, we show that the dissipative gap scales with entanglement entropy exactly as predicted by our bound. Moreover, we show analytically that the relaxation of a Haar-random initial state follows the same scaling as predicted by the bound. Our general reverse engineering of local dissipation compatible with a target entangled state could have a variety of other interesting applications [38].

One potential application of recent interest is the design of open quantum systems that are able to simulate finite-temperature states of many-body systems (often called quantum Gibbs samplers) [38–41]. Our technique could be used to prepare the purified thermofield double (TFD) state, which allows one to probe finite-temperature properties. Another possible use is given in Ref. [42], where our technique would be able to prepare an entangled state for optimal multiparameter metrology.

This paper is organized as follows. In Sec. II, we establish our general setup, while in Sec. III we provide a rigorous statement of our main results. In Sec. IV, we show how to reverse engineer a class of local dissipative dynamics that all stabilize a given target entangled state. We combine this with random matrix theory to show that typical relaxation times scale with entanglement entropy exactly as predicted by our bound. In Sec. V, we show that the spectra of random Lindbladians exhibit a bulk gap along with isolated midgap state(s), which are responsible for all of the slow dynamics.

II. SETUP AND DEFINITIONS

A. Maximally entangled states

We work throughout with systems having a tensor-product Hilbert space $\mathcal{H} = \mathcal{H}_A \otimes \mathcal{H}_B$ (with dim $\mathcal{H}_{A,B} = N_{A,B} < \infty$) and we will be interested in pure states with entanglement between subsystems A and B. Unless otherwise stated, we will assume that $N_A = N_B \equiv N$. Any state $|\psi\rangle \in \mathcal{H}$ admits a Schmidt decomposition

$$|\psi\rangle = \sum_{i=1}^{\min(N_A,N_B)} \sqrt{p_i} |i\rangle_A \otimes |i\rangle_B, \qquad (1)$$

where the Schmidt coefficients $\sqrt{p_i}$ are taken to be real and positive without loss of generality throughout. A *maximally entangled state* for our bipartition is

any state with uniform Schmidt coefficients, i.e., $\sqrt{p_i} = [\min(N_A, N_B)]^{-1/2} \, \forall i$.

The bipartite entanglement of $|\psi\rangle$ can be characterized by the Renyi-α entropy between subsystems A and B:

$$S^{(\alpha)}(|\psi\rangle) = \frac{1}{1-\alpha} \log \sum_i p_i^\alpha. \qquad (2)$$

For a maximally entangled state $|\psi\rangle_{\max}$ (letting $N_A = N_B = N$), this gives

$$S^{(\alpha)}(|\psi\rangle_{\max}) = \log N. \qquad (3)$$

B. Open Markovian dynamics and time scales

Our overarching goal is to connect steady-state entanglement to dynamics. We will focus exclusively on systems the open-system dynamics of which are described by a Markovian master equation in GKSL) form [12,13]. Letting $\hat{\rho}$ be the density matrix of the system, we have

$$\partial_t \hat{\rho} = -i[\hat{H}, \hat{\rho}] + \sum_{\mu=1}^{M} \mathcal{D}[\hat{L}_\mu]\hat{\rho} \equiv \hat{\mathcal{L}}\hat{\rho}, \qquad (4)$$

$$\mathcal{D}[\hat{L}_\mu]\hat{\rho} \equiv \hat{L}_\mu \hat{\rho} \hat{L}_\mu^\dagger - \frac{1}{2}\left\{ \hat{L}_\mu^\dagger \hat{L}_\mu, \hat{\rho} \right\}, \qquad (5)$$

where the Hermitian operator $\hat{H}$ is the Hamiltonian and the M jump operators $\hat{L}_\mu$ parametrize the nonunitary evolution. We will refer to the superoperator $\hat{\mathcal{L}}$ as the Lindbladian. As we discuss below, we consider situations in which subsystems A and B are physically separated and only interact via local couplings to common dissipative environments. As a result, we require all jump operators to have the form

$$\hat{L}_\mu = \hat{A}_\mu \otimes \mathbb{1} + \mathbb{1} \otimes \hat{B}_\mu. \qquad (6)$$

Every Lindbladian will have at least one steady-state solution $\hat{\rho}_{\rm ss}$, defined by $\hat{\mathcal{L}}\hat{\rho}_{\rm ss} = 0$. Our interest here is in systems that have a pure steady state; the goal is to connect the entanglement of the steady state to dynamical time scales. We say that $\hat{\mathcal{L}}$ has a maximally entangled steady state if there exists a state $|\psi\rangle$ such that $S^{(\alpha)}(|\psi\rangle) = \log N$ and $\hat{\mathcal{L}}(|\psi\rangle\langle\psi|) = 0$. A steady state is unique if and only if every initial condition tends toward the steady state in the long-time limit.

In most cases, we will be interested in systems in which $\hat{\mathcal{L}}$ is diagonalizable and can be written as $\hat{\mathcal{L}} = \sum_{\alpha=0}^{N^4-1} \lambda_\alpha |r_\alpha\rangle\rangle\langle\langle l_\alpha|$. (Here and throughout, the double-bracket notation $|\hat{\rho}\rangle\rangle$ represents a vectorized density matrix.) The complete set of dissipative rates is given by the real parts of the eigenvalues $\{\lambda_\alpha\}$. We will work with

the convention that $0 = \lambda_0 \geq \mathrm{Re}\lambda_1 \geq \cdots \geq \mathrm{Re}\lambda_{N^4-1}$ [43]. We define the dissipative gap

$$\Delta = -\mathrm{Re}\lambda_1. \qquad (7)$$

C. Locality in bipartite Lindbladians

When proving an area law for the ground states of gapped 1D systems, one has to first imbue the Hamiltonian with a meaningful notion of locality. Similarly, we must identify a relevant notion of locality in our open-system dynamics. To that end, we assume that subsystems A and B are physically separated and only interact via local couplings to common extended Markovian reservoirs (see Fig. 1). For example, one might consider groups of qubits decaying into a common waveguide or groups of atoms interacting with a common cavity mode. The locality of this setup means that before eliminating the environment to generate our master equation, its interaction with the system will be described by a Hamiltonian of the form

$$\hat{H}_{\rm int} = \sum_{\mu=1}^{M'} \hat{R}_{A,\mu} \otimes \hat{\bar{A}}_\mu \otimes \mathbb{1} + \hat{R}_{B,\mu} \otimes \mathbb{1} \otimes \hat{\bar{B}}_\mu + \text{H.c.,} \quad (8)$$

where μ indexes interactions with the reservoir(s) and $\hat{R}_{A,\mu}$ and $\hat{R}_{B,\mu}$ are reservoir operators localized near either the A or the B subsystem, respectively. Correspondingly, $\hat{\bar{A}}_\mu$ $(\hat{\bar{B}}_\mu)$ are subsystem A (B) operators. Note crucially that A and B *only* interact via their common coupling to the environment.

Assuming now that the reservoir(s) is Markovian, we can eliminate it in the usual manner (see, e.g., Refs. [44,45]) to generate a GKSL master equation for the dynamics of $A + B$ with the constrained form of Eqs. (4)–(6) (for more details, see Appendix F). In particular, each jump operator $\hat{L}_\mu$ is the sum of an A and a B operator as given in Eq. (6), where $\hat{A}_\mu$ and $\hat{B}_\mu$ are local A, B operators that depend on $\hat{\bar{A}}_\mu$ and $\hat{\bar{B}}_\mu$ as well as reservoir properties. Even with this constraint, we have an extremely general problem. We can still have arbitrary local dissipative processes (i.e., set either $\hat{A}_\mu$ or $\hat{B}_\mu$ to 0), as well as all forms of correlated Markovian dissipation relevant to physically separated systems. Moreover, we place no constraints on the Hamiltonian $\hat{H}$ in Eq. (4) (as there could be arbitrary bath-induced Hamiltonian interactions between A and B).

D. Connection to measurement-feedback dynamics

The general setup described by Eqs. (4) and (5) is also directly relevant to describing dynamics where A and B interact via locality-constrained continuous measurement and feedforward (MFF) processes [46–48]. In particular,

this constrained form describes the unconditional dynamics arising from a MFF protocol where one measures *sums* of A and B quantities and then uses the results to apply local feedback control to each subsystem. To be explicit, consider the unconditional dynamics generated by making a weak continuous measurement of a Hermitian observable $\hat{M}$ and then using the measurement record to drive another Hermitian quantity $\hat{F}$. In the limit where delay can be neglected, the theory of weak continuous measurement shows that the unconditional state (i.e., averaged over all possible measurement outcomes) evolves as [49]

$$\partial_t \hat{\rho} = \mathcal{D}[\hat{M}]\hat{\rho} + \mathcal{D}[\hat{F}]\hat{\rho} - i[\hat{F}, \{\hat{M}, \hat{\rho}\}]$$
$$= \mathcal{D}[\hat{F} - i\hat{M}]\hat{\rho} - \frac{i}{2}[\{\hat{F}, \hat{M}\}, \hat{\rho}]. \qquad (9)$$

As long as both $\hat{M}$ and $\hat{F}$ are sums of local operators, we have a master equation that obeys the general form of Eqs. (4)–(6). For example, we could take

$$\hat{M} = \frac{i}{2}(\hat{A} - \hat{A}^\dagger + \hat{B} - \hat{B}^\dagger), \qquad (10)$$

$$\hat{F} = \frac{1}{2}(\hat{A} + \hat{A}^\dagger + \hat{B} + \hat{B}^\dagger). \qquad (11)$$

In this case, $\hat{F} - i\hat{M} = \hat{A} + \hat{B}$, implying that the dissipator in Eq. (9) has the required form of Eq. (6) (while the last term in Eq. (9) is a Hamiltonian interaction that is always allowed).

Given this connection, the entanglement-time bounds that we prove below directly constrain locality-constrained measurement-plus-feedback protocols. Moreover, we stress that while we have formulated the measurement-plus-feedback protocol without any additional Hamiltonian interactions, any Hamiltonian can always be added in without any change to our results.

III. BOUND STATEMENT

A. Maximally entangled steady states cannot be reached by Markovian dynamics

It is well known that dissipative dynamics having the form of Eqs. (4)–(6) can be used to stabilize pure entangled states. Examples include the dissipative stabilization of bosonic two-mode squeezed states [50–52], qubit Bell pairs [22,29,36], and even more exotic states of matter in spin chains [32,36]. Our first result is to show that all such protocols are highly constrained. If a Lindbladian $\hat{\mathcal{L}}$ of the form given in Eqs. (4)–(6) has a pure *maximally* entangled steady state $|\psi\rangle$ (i.e., $\hat{\mathcal{L}}|\psi\rangle\langle\psi| = 0$), then this state is necessarily dynamically isolated: the projector $|\psi\rangle\langle\psi|$ becomes a conserved quantity, implying that the dissipative dynamics will never relax an arbitrary initial state into

this entangled state. This necessarily implies the existence of multiple steady states and the closing of the dissipative gap. Our result here holds irrespective of further details (e.g., the Hilbert-space dimension, the number of jump operators, the form of the $\hat{A}_\mu$ and $\hat{B}_\mu$ operators, the form of $\hat{H}$, etc.).

To establish this result, note first that as $|\psi\rangle$ is a pure steady state, we necessarily have [34]

$$[\hat{H}, |\psi\rangle\langle\psi|] = \hat{L}_\mu|\psi\rangle = 0, \qquad (12)$$

i.e., it is an eigenstate of the Hamiltonian and a dark state of each jump operator. Within the quantum jumps interpretation of our master equation [49], the dark-state conditions imply that if the system is in the state $|\psi\rangle$, there is zero probability of a quantum jump evolving it into a different state.

The fact that $|\psi\rangle$ is also maximally entangled leads to a second, even stronger, constraint: there will also be zero probability that a quantum jump from an arbitrary initial state $|\phi\rangle$ will produce a state with nonzero overlap with $|\psi\rangle$. To see this explicitly, we define the unnormalized "absorbing state" associated with each jump operator $\hat{L}_\mu$ to be $|\tilde{\psi}_\mu\rangle \equiv \hat{L}_\mu^\dagger|\psi\rangle$. The probability that a quantum jump induced by $\hat{L}_\mu$ will result in some initial state $|\phi\rangle$ having overlap with $|\psi\rangle$ is then $|\langle\psi|\hat{L}_\mu|\phi\rangle|^2 = |\langle\tilde{\psi}_\mu|\phi\rangle|^2$. Using the fact that $|\psi\rangle$ is a dark state, we have

$$\langle\tilde{\psi}_\mu|\tilde{\psi}_\mu\rangle = \langle\psi|\hat{L}_\mu\hat{L}_\mu^\dagger|\psi\rangle = \langle\psi|[\hat{L}_\mu, \hat{L}_\mu^\dagger]|\psi\rangle$$
$$= \langle\psi|[\hat{A}_\mu, \hat{A}_\mu^\dagger] \otimes \mathbb{1}|\psi\rangle + \langle\psi|\mathbb{1} \otimes [\hat{B}_\mu, \hat{B}_\mu^\dagger]|\psi\rangle. \qquad (13)$$

Next, as $|\psi\rangle$ is also a maximally entangled state, an explicit calculation shows that the above expression is proportional to $\text{tr}[\hat{A}_\mu, \hat{A}_\mu^\dagger] + \text{tr}[\hat{B}_\mu, \hat{B}_\mu^\dagger] = 0$ when $N_A = N_B$ (see Appendix A). Hence, there is zero probability of a quantum jump moving population into the entangled steady state $|\psi\rangle$. The vanishing of $|\tilde{\psi}_\mu\rangle$ also implies that the "no-jump" evolution described by $\hat{H}_{\text{eff}} = \hat{H} - (i/2)\sum_\mu \hat{L}_\mu^\dagger\hat{L}_\mu$ will never increase the population of $|\psi\rangle$. We thus have established our key result: the population of the maximally entangled steady state $|\psi\rangle$ will never change in time and hence, even given infinite time, dissipative preparation of the steady state $|\psi\rangle$ is impossible.

We can also establish this result rigorously using the notion of a strong symmetry of a Lindbladian [53]. In Eq. (13), it is shown that for each jump operator, $\hat{L}_\mu^\dagger|\psi\rangle = 0$. Given that $|\psi\rangle$ is also a pure steady state, it immediately follows that

$$[\hat{P}, \hat{L}_\mu] = [\hat{P}, \hat{H}] = 0, \qquad (14)$$

where $\hat{P} = |\psi\rangle\langle\psi|$. This implies that $\hat{P}$ (the projector onto $|\psi\rangle$) generates a strong symmetry of $\hat{\mathcal{L}}$ and describes a

dynamically conserved charge. It thus separates the full Hilbert space into two dynamically isolated subspaces, namely, $|\psi\rangle$ and its orthogonal complement. It also tells us that there must be steady-state degeneracy (i.e., at least one steady state orthogonal to $|\psi\rangle$) and hence a vanishing of the dissipative gap. Our result here generalizes the discussion of Ref. [30], which discusses this phenomenon in a specific two-qubit Lindbladian, where the conserved quantity reduces to total angular momentum. Our generalization shows that this phenomenon occurs in an extremely broad class of systems (including systems in the truly many-body limit) and that the conserved quantity is the population of the entangled steady state itself.

B. Universal time-entanglement trade-off

We now establish the second main result of this work: a fundamental trade-off in our locality-constrained dissipative dynamics between the amount of pure steady-state entanglement and the time scales associated with dissipative stabilization. We find that a rigorous bound that implies increased steady-state entanglement leads to longer relaxation times (with the time scale diverging for maximal entanglement, as demonstrated above).

To formulate these ideas, we again consider a Lindbladian $\hat{\mathcal{L}}$ of the form in Eqs. (4)–(6), which has a pure steady state $\hat{\rho}_{ss} \equiv |\psi\rangle\langle\psi|$. We now allow $\hat{\rho}_{ss}$ to have an arbitrary amount of entanglement. Consider the time evolution of an arbitrary initial state under $\hat{\mathcal{L}}$, with the time-dependent density matrix denoted as $\hat{\rho}_t$. We are interested in how this state relaxes toward $\hat{\rho}_{ss}$ and thus we consider the fidelity $F(t)$ between these states:

$$F(t) = \left(\text{tr}\sqrt{\sqrt{\hat{\rho}_{ss}}\hat{\rho}_t\sqrt{\hat{\rho}_{ss}}} \right)^2. \quad (15)$$

Relaxation of an initial trivial state to the entangled steady state corresponds to $F(t)$ evolving from approximately 0 at $t = 0$ to approximately 1 at some finite time $t \sim \tau_{rel}$.

To formulate our result, consider the product basis defined by the Schmidt decomposition of our pure steady state given in Eq. (1). To fix a single time scale for the problem, we will nondimensionalize the jump operators by pulling out an overall scale factor with units of frequency. This allows us to differentiate the role that entanglement plays in the dynamics from the more trivial role that the overall magnitude of the Lindbladian plays. That is, we will define $|\hat{A}_\mu| \equiv \sqrt{\kappa_\mu}$ to be the magnitude of the largest matrix element of $\hat{A}_\mu$ in the Schmidt basis, so that we can write each jump operator as

$$\hat{L}_\mu = \sqrt{\kappa_\mu}\left(\frac{\hat{A}_\mu}{|\hat{A}_\mu|} \otimes \mathbb{1} + \mathbb{1} \otimes \frac{\hat{B}_\mu}{|\hat{A}_\mu|} \right) \equiv \sqrt{\kappa_\mu}\hat{\tilde{L}}_\mu, \quad (16)$$

where $\hat{\tilde{L}}_\mu$ is unitless and κ_μ has the units of a rate. From here, we define the average rate $\overline{\kappa} = 1/M \sum_{\mu=1}^{M} \kappa_\mu$. We will go on to show that this average rate $\overline{\kappa}$ appears naturally in the models considered and sets an overall time scale. Turning to the steady state $\hat{\rho}_{ss} = |\psi\rangle\langle\psi|$, we use $S_{ss}^{(2)}$ to denote its Renyi-2 entanglement entropy [cf. Eq. (2)] and define $\sqrt{p_{min}}$ to be its smallest Schmidt coefficient.

Finally, we introduce the scaled entanglement $\mathcal{E}_2$, a measure for the steady-state entanglement based on $S^{(2)}$ that varies from 0 (no entanglement) to 1 (maximal entanglement):

$$\mathcal{E}_2 \equiv \frac{1}{1 - 1/N}\left(1 - e^{-S_{ss}^{(2)}} \right)$$

$$= \frac{1}{1 - 1/N}\left(1 - \sum_{j=1}^{N} p_j^2 \right). \quad (17)$$

With these definitions in hand, we can state our key result: the growth of the fidelity $F(t)$ is rigorously bounded by a rate, the value of which is directly proportional to the entanglement deficit of the steady state. Assuming first that $p_{min} > 0$, we have

$$|F(t) - F(0)| \leq \Gamma_{max}t, \quad (18a)$$

$$\frac{\Gamma_{max}}{M\overline{\kappa}} = \sqrt{2}(N-1)(p_{min})^{-1}(1 - \mathcal{E}_2), \quad (18b)$$

where $N \equiv N_A = N_B$. A full proof of this result is presented in Appendix A. We see that the growth of the fidelity toward 1 is bounded by the rate Γ_{max}, which in turn decreases linearly with the scaled entanglement $\mathcal{E}_2$. For a maximally entangled state ($\mathcal{E}_2 = 1$), Γ_{max} vanishes, thus recovering the result of Sec. III A: $F(t)$ is time independent in this case and no dynamical stabilization of the entangled steady state is possible. For more general cases, our result provides a lower bound on the relaxation time τ_{rel}: $\tau_{rel} \geq 1/\Gamma_{max} \propto 1/(1 - \mathcal{E}_2)$. At a heuristic level, for $\mathcal{E}_2 < 1$ we do not have a perfect strong symmetry and conserved quantity as in the maximal-entanglement case [cf. Eq. (14)]. Nonetheless, there is an "almost" conserved quantity that relaxes slowly, leading to very slow relaxation to the steady state. This is discussed in more detail in Appendix C.

The bound in Eq. (18) is for the case in which the steady-state reduced density matrix of each subsystem is full rank; it clearly has no utility in the case in which p_{min} is zero or extremely small. In these cases, an analogous, more useful, bound can be derived that again constrains relaxation time scales in terms of the steady-state entanglement deficit. The bound still has the form of Eq. (18a) but the rate Γ_{max}

is replaced by $\Gamma'_{\max}$ (see Appendix A):

$$\frac{\Gamma'_{\max}}{\sqrt{2(N^3 - N^2)}} = \left[\left(\sum_{\mu=1}^{M} |\hat{A}_\mu| \right)^2 + \left(\sum_{\mu=1}^{M} |\hat{B}_\mu| \right)^2 \right]$$
$$\times (1 - \mathcal{E}_2)^{1/2} . \quad (19)$$

The rate in this bound is still decreases monotonically with increasing scaled entanglement $\mathcal{E}_2$ and vanishes as one approaches maximal entanglement $\mathcal{E}_2 = 1$.

Finally, the bounds discussed here constrain the relaxation of *any* state toward the entangled pure steady state. It thus sets a speed limit for even the optimal cases, where one has a fast-relaxing state. It is interesting to instead ask about the relaxation of a *typical* state toward the entangled steady state. We can also derive a general bound that applies to this situation. Consider that at some time t we have a Haar-random pure state of our system, $\hat{\rho}_t = \hat{U}|\phi_0\rangle\langle\phi_0|\hat{U}^\dagger$, where $\hat{U}$ is a Haar-random unitary and $|\phi_0\rangle$ is some arbitrary fixed state. We can then derive a rigorous bound on the instantaneous change in the average fidelity $F(t)$ (see Appendix B):

$$\int_{\text{Haar}} |\partial_t F| \, d\hat{U} \leq 2M\overline{\kappa} \frac{N - 1}{N^2} (p_{\min})^{-1} (1 - \mathcal{E}_2) . \quad (20)$$

We again find the same scaling with the scaled entanglement but now with a smaller N-dependent prefactor.

Finally, the same physics that leads to the bounds in Eqs. (18)–(20) can also be used to bound the mixing time of the Lindbladian [54], a standard time-scale metric for dissipative dynamics. This involves using inequalities between quantum fidelity and the trace distance [55]. Explicitly, if we define

$$t_{\text{mix}}(\epsilon) = \inf\{t > 0 \mid \forall\hat{\rho}, d_{\text{tr}}(e^{\hat{\mathcal{L}}t}\hat{\rho}, \hat{\rho}_{\text{ss}}) \leq \epsilon\}, \quad (21)$$

where d_{tr} is the trace distance, then we show (see Appendix A) that

$$t_{\text{mix}}(\epsilon) \geq \frac{1 - \epsilon}{\Gamma_{\max}} = \frac{(1 - \epsilon)M\overline{\kappa}p_{\min}}{\sqrt{2}(N - 1)}(1 - \mathcal{E}_2)^{-1}, \quad (22)$$

where $\Gamma_{\max}$ is the rate introduced in Eq. (18).

Equations (18)–(20) and Eq. (22) are key results of this work. They provide a unifying explanation for phenomena seen in specific studies of a variety of different dissipative systems, all of which have witnessed an extreme slow-down of the dynamics as parameters have been tuned to increase the entanglement of the dissipative steady state [29,30,36]. Moreover, while they have been formulated for the case in which both systems have the same Hilbert-space dimension, $N_A = N_B$, they can be easily extended to the case in which this is not true. In this more general case,

one can always map the problem to the case in which the dimensions are equal but one system is completely decoupled from some of its levels. One could then directly apply the bound given in Eq. (19). More importantly, such a setup is, by definition, never close to being maximally entangled by our definition (as it is not exploiting the full Hilbert space; for more details, see Appendix A).

IV. MANY-BODY RANDOM LINDBLADIANS

While our entanglement-time bound in Eq. (18) is rigorous, it only provides a lower bound on the relaxation times. There is no *a priori* reason to assume that this bound is tight or that it even qualitatively captures how the relaxation time scales vary in a typical system. For example, it could be that the relaxation times diverge with increasing entanglement in a manner that is much worse than the predictions of our bound.

To address these issues, in this section we study relaxation times in an ensemble of random Lindbladians having the form of Eqs. (4)–(6), all of which have a pure steady state having some *fixed* value of the scaled entanglement $\mathcal{E}_2$ [cf. Eq. (17)]. We can then ask about the statistics of relaxation times in this ensemble and how they vary as we change the steady-state entanglement.

A. Reverse engineering dissipative dynamics compatible with a target entangled state

To proceed, we consider a system with fixed local Hilbert-space dimension N for each subsystem and start by picking a particular (perhaps randomly chosen) pure steady state $|\psi\rangle$ specified by its Schmidt coefficients $\sqrt{p_j}$ [cf. Eq. (1)]. These coefficients can be used to define a single system operator $\hat{\Psi}$, which is simply the square root of the reduced steady-state density matrix for each subsystem:

$$\hat{\Psi} \equiv \sum_i \sqrt{p_i}|i\rangle\langle i| = \sqrt{\hat{\rho}_A} = \sqrt{\hat{\rho}_B}, \quad (23)$$

where the $|i\rangle$ are states in the Schmidt basis for the entangled state $|\psi\rangle$ and $\hat{\rho}_A = \text{tr}_B|\psi\rangle\langle\psi|$, $\hat{\rho}_B = \text{tr}_A|\psi\rangle\langle\psi|$. In what follows, we assume that all Schmidt coefficients are nonzero, i.e., that $\hat{\Psi}$ is full rank.

The next step is to construct dissipative dynamics of the form of Eqs. (4)–(6) that have the chosen pure state $|\psi\rangle$ as a steady state. We focus on the simple case in which there is no Hamiltonian and thus the problem reduces to finding one or more jump operators $\{\hat{L}_\mu\}$ such that $\hat{L}_\mu|\psi\rangle = 0$, and where each jump operator is the sum of an operator acting on just one subsystem: $\hat{L}_\mu = \hat{A}_\mu + \hat{B}_\mu$. Our approach is to first pick arbitrary system-A operators $\hat{A}_\mu$ for each jump operator. The dark-state conditions then uniquely determine the form of the corresponding system-B operator in each $\hat{L}_\mu$. Letting A_μ, B_μ, and Ψ_μ denote the $N \times N$ matrix

representation of these operators in the Schmidt basis, we have

$$(\hat{A}_\mu \otimes \mathbb{1} + \mathbb{1} \otimes \hat{B}_\mu)|\psi\rangle = 0 \implies B_\mu = -\Psi A_\mu^T \Psi^{-1}. \quad (24)$$

Our construction here provides an extremely general way to construct a large number of dissipative dynamics that will stabilize a particular chosen pure entangled steady state. The construction guarantees that for a particular jump operator, the operators $\hat{A}_\mu$ and $-\hat{B}_\mu$ are isospectral. As a result, the kernel of a single jump operator $\hat{L}_\mu$ necessarily has a dimension $\geq N$ (see Appendix A). Having a unique steady state will thus require at least two jump operators (chosen so that the desired steady state $|\psi\rangle$ spans the intersection of their kernels). Alternatively, one could remedy this problem by introducing an appropriate Hamiltonian to the dynamics.

We note that the construction here (where B operators can be viewed as the modular conjugation of A operators) has a close connection to certain formulations of quantum detailed balance (i.e., Kubo-Martin-Schwinger (KMS) detailed balance [56,57] and hidden-time reversal symmetry [58]), as well as to the theory of coherent quantum absorbers [21,59]. The construction is also reminiscent of the construction of the Petz recovery map [60] and formal constructions of Hamiltonians that have thermofield double states as their ground state [61].

B. Entanglement-time trade-offs and dissipative gap scaling in random many-body dissipative dynamics

We now use our state-to-dynamics construction to assess whether the general time-entanglement bound in Eq. (18) tells us anything about typical relaxation times. For a given chosen steady-state entanglement $\mathcal{E}_2$, we first construct an ensemble of entangled pure states $|\psi_\alpha\rangle$ all having the same $\mathcal{E}_2$. For each state, we then use our construction to generate a random Lindblad master equation having two jump operators that will stabilize this state. This involves first picking two random $N \times N$ matrices, A_1 and A_2, and then using Eq. (24) to pick the corresponding B matrices. These matrices then define the jump operators $\hat{L}_1$ and $\hat{L}_2$. We draw each A matrix from the complex random Ginibre ensemble: each matrix element is a Gaussian random variable with $\mathbb{E}[(A_\mu)_{ij}] = 0$ and $\mathbb{E}[(A_\mu)_{ij}^*(A_\nu)_{kl}] = \sigma^2 \delta_{\mu\nu}\delta_{ik}\delta_{jl}$. As we have no Hamiltonian contribution to our dynamics, the variance σ^2 plays no role except setting an overall time scale for the dynamics. That is to say, we can always choose to set $\sigma = 1$ by absorbing it into κ_μ as defined in Eq. (16). In this way, we can separate the dimensionful quantity κ_μ from the dimensionless slow-down due to the entanglement entropy. Another way of putting this is to observe that if we let $\hat{\mathcal{L}}_\sigma$ be a Lindbladian sampled from the random ensemble where each matrix element of

A has variance σ, then $\hat{\mathcal{L}}_\sigma = \sigma^2 \hat{\mathcal{L}}_{\sigma=1}$. Hence, if we normalize the Lindbladian to fix a time scale, the factors of σ^2 drop out and can therefore be set to unity without loss of generality. Note that this is only true because there is no Hamiltonian; otherwise, σ would control the strength of the dissipative dynamics relative to the coherent dynamics.

In Fig. 2, we show results obtained by numerically implementing this procedure for system sizes N ranging from 4 to 10. We plot the dissipative gap [cf. Eq. (7)] for each constructed random Lindbladian, as a function of their steady-state entanglement $\mathcal{E}_2$. We stress that each realization here involves both randomly constructing a pure entangled steady state and dissipative dynamics that will stabilize this state. The dissipative gap Δ characterizes the slowest relaxation process in our system and hence we might expect that $\Delta \sim \Gamma_{\text{max}}$, where Γ_{max} is the rate appearing in our general bound Eq. (18). We see that there is a striking linear scaling of the average dissipative gap with $\mathcal{E}_2$, $\Delta \propto 1 - \mathcal{E}_2$. This is exactly the dependence predicted by our general bound for Γ_{max}. While the prefactor of the scaling does not match the system-size dependence predicted by our bound, we see that the general trade-off between entanglement and relaxation times in this class of unstructured many-body Lindbladians is quantitatively in agreement with Eq. (18).

Further, these results are not contingent on our use of the complex Ginibre ensemble to construct our random dissipators. As shown in Appendix B, constructions based on other, physically motivated, random ensembles also show analogous scaling.

Turning to the prefactor of the average dissipative gap scaling with $1 - \mathcal{E}_2$, the bound states that it cannot grow faster than N^2. However, as shown in Fig. 2(b), we numerically find that, for randomly sampled Lindbladians, it appears to be independent of N. Further, we see that the fluctuations of the dissipative gap about its average decrease significantly even for modest increases in N. At this point, we stress that this does not imply that the bound is not tight, as it must account for *all possible Lindbladians*, whereas in Fig. 2, we consider only the more constrained set of *average* or *random Lindbladians*. In fact, in Sec. IV C, we will give a specific example of a system that relaxes much more quickly than the Haar-random examples but still satisfies the bound. To truly prove whether or not the bound is tight requires either finding a tighter bound or finding a model system that saturates it, which we leave to future works.

However, we can analytically show that the Haar-random case should have a prefactor that is independent of system size. First, define the deviation from maximal entanglement:

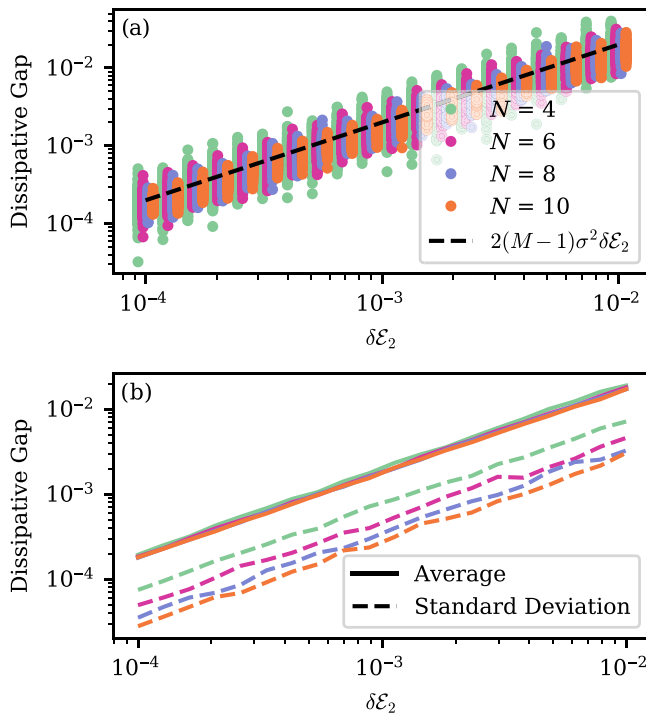$$\delta\mathcal{E}_2 \equiv \frac{N-1}{N}(1 - \mathcal{E}_2). \quad (25)$$

FIG. 2. (a) The dissipative gap of random Lindbladians stabilizing a random pure state with a fixed entanglement $\delta\mathcal{E}_2$ [cf. Eq. (25)], for varying system size, constructed using Eq. (24). Recall that $\delta\mathcal{E}_2$ decreases monotonically with increasing entanglement and is zero for a maximally entangled state. Here, each A_μ matrix that is used to construct our dissipators is sampled from the Ginibre ensemble of random matrices with variance σ. For each system size and entanglement value, we plot results for 100 random Lindbladians. Different values of N are offset horizontally to avoid overlap. (b) The average and standard deviation of data in (a) for a fixed system size and entanglement. The average gap is $2(M-1)\sigma^2\delta\mathcal{E}_2$ and is independent of system size. The standard deviation also scales linearly with $\delta\mathcal{E}_2$ and falls off as N increases.

Then, assume that we have M random dissipators constructed as above and that for a fixed $\mathcal{E}_2$ the Schmidt coefficients p_j are chosen randomly subject to normalization $\sum_j p_j = 1$ and $\mathcal{E}_2$ is fixed [cf. Eq. (17)]. To leading order in $\delta\mathcal{E}_2$, one can show (see Appendix B) that

$$\mathbb{E}\left[\int_{\text{Haar}} |\partial_t F| \, dU\right] = 2M\sigma^2\delta\mathcal{E}_2, \quad (26)$$

where $\mathbb{E}[\bullet]$ is an average both over matrices A_μ as well as the Schmidt coefficients p_j. We now have a scaling of a typical relaxation rate that is still proportional to $(1 - \mathcal{E}_2)$ but with an N-independent prefactor.

We expect that Eq. (26) will give a good estimate of the dissipative gap Δ, except for the correction that $M \to M - 1$. The reason for this is that, due to the condition in Eq. (24), a single jump operator generates N steady states and so the dissipative gap is by definition zero when $M =$

1. Despite this, the dynamics can still increase the fidelity to the chosen steady state; hence Eq. (26) is nonzero even when $M = 1$. To account for this difference between the dissipative gap and the rate of change of the fidelity, we expect that the average dissipative gap scales as

$$\mathbb{E}[\Delta] = 2(M-1)\sigma^2\delta\mathcal{E}_2. \quad (27)$$

This is in good agreement with the behavior of the average dissipative gap shown in Fig. 2.

Note that for the Lindbladians considered here, we find that the dissipative gap accurately predicts long-time relaxation to the steady state. It is well known that there exist examples where this correspondence can fail [62–64], e.g., in systems exhibiting so-called "skin effects" (see, e.g., Refs. [65–71]). Note that even for cases in which the dissipative gap is not reflective of relaxation, our general bound in Eq. (18) remains valid: it directly constrains the dynamics of the fidelity $F(t)$ (a physically observable quantity), without any assumptions on how the dissipative gap is related to the decay of observables.

C. Typical versus best-case relaxation rates

As noted above, it is unclear whether or not the bound stated in Eq. (18) is tight, as the random systems sampled from the given distribution seem to relax roughly N^2 times more slowly than the fastest-possible rate predicted by the bound. However, we stress that there is nothing contradictory: the bound in Eq. (18) must account for all possible Lindbladians subject to the locality constraint, whereas in the random case, the systems are much less general.

For example, by adding back in more structure than is present in the randomly sampled Lindbladians, we can construct a model that, while not saturating the bound, does have a prefactor that is $\mathcal{O}(N)$, in between the one given in the bound and the Haar-random case.

Consider a Lindbladian $\hat{\mathcal{L}}_1$ acting on a Hilbert space with local dimension d, which has a steady-state Renyi-2 entanglement entropy $S_1^{(2)}$ and a dissipative gap Δ_1. We can enlarge the Hilbert space in a trivial way by tensoring together n copies of the same steady state, which evolve under the Lindbladian

$$\hat{\mathcal{L}} = \sum_{i=1}^{n} \mathbb{1}^{\otimes i-1} \otimes \hat{\mathcal{L}}_1 \otimes \mathbb{1}^{\otimes n-i}. \quad (28)$$

The steady-state entanglement entropy (taking a bipartition that splits each copy) is now $S_{\text{ss}}^{(2)} = nS_1^{(2)}$ by additivity. Thus, the deviation of the scaled entanglement from its maximum value scales as

$$1 - \mathcal{E}_2 = \frac{N}{N-1}\left(e^{-S_{\text{ss}}^{(2)}} - \frac{1}{N}\right) \quad (29)$$

$$= \frac{1}{1-d^{-n}}\left(e^{-nS_1^{(2)}} - d^{-n}\right), \quad (30)$$

which decays exponentially with n. It thus follows from Eq. (26) that the instantaneous rate of change in fidelity between a Haar-random state and the steady state is decaying *exponentially* in the number of copies n. However, by construction, the dissipative gap in this system is independent of n, suggesting no slow-down with increasing system size. This lack of slow-down is, however, consistent with the larger prefactor in our more general bound in Eq. (18).

This example shows that a general bound must have a prefactor that grows with N at least as $\mathcal{O}(N/\log(N))$. The large deviation between this example and the Haar-random models can be attributed to the highly structured form of the Lindbladian. Stated succinctly, the eigenvectors of the Lindbladian are now very far from being related to Haar-random states. All of the eigenvectors of Eq. (28) are completely unentangled between copies and so approximating them with a Haar-random state is unsuccessful.

V. BEYOND THE SLOWEST RELAXATION RATE: THE STRUCTURE OF THE LINDBLADIAN SPECTRA

A. Bulk gap and midgap states

The results of Sec. IV show that for random unstructured dissipative dynamics that are locality-constrained and which have a pure steady state, the scaling of the dissipative gap with steady-state entanglement matches the predictions of our general bounds in Eqs. (18) and (20). In this section, we turn to another question: does increasing steady-state entanglement only lead to the formation of at most a handful of slow-relaxation modes or does it imply that an extensive number of relaxation modes become slow? This is a question about the full spectrum of our Lindbladian and not just the dissipative gap. Through numerical investigation, we find that the first scenario holds: strong steady-state entanglement leads to the formation of a unique slow mode, whereas the vast majority of relaxation modes exhibit no slow-down. We find that for a variety of different random Lindbladians, the spectrum of relaxation rates exhibit what we term a "bulk gap," where almost every mode has an $\mathcal{O}(\overline{\kappa})$ decay rate regardless of the slow-down associated with large steady-state entanglement. However, there also always exists a single isolated "midgap" state, which decays extremely slowly and is responsible for all of the long-time slow dynamics.

To provide context for this result, we first recall known results for the spectral properties of completely unstructured random Lindbladians (i.e., dynamics that do not have the locality and purity constraints of our general setting). Consider a general Lindbladian for a system with an N-dimensional Hilbert space:

$$\hat{\mathcal{L}}\hat{\rho} = \sum_{\mu,\nu=1}^{N} K_{\mu\nu}\left(\hat{F}_\mu\hat{\rho}\hat{F}_\nu^\dagger - \frac{1}{2}\left\{F_\nu^\dagger\hat{F}_\mu, \hat{\rho}\right\}\right), \quad (31)$$

where $K_{\mu\nu}$ is the complex positive semidefinite $N \times N$ "Kossakowski matrix." We take $K = NGG^\dagger/\mathrm{tr}(GG^\dagger)$, with the matrix G sampled from the complex Ginibre ensemble (unit variance of matrix elements). The operators $\{\hat{F}_\mu\}$ form an orthonormal traceless basis of SU(N).

For this general setup, it can be shown that the average dissipative gap scales as $1 - 2/N$ [72]. For large N, the average gap becomes N independent, a scaling that will match almost all relaxation modes in our more structured dissipative problem. However, the additional constraints that we impose in our general setup (entangled pure steady state, local form of dissipators) lead to the formation of a single extremely slow mode as entanglement is increased, i.e., a "midgap state" [see Fig. 4(a)]. It is this single slow mode that is responsible for the slow relaxation described by our bounds. It is also interesting to note that the midgap state(s) are purely a result of the entanglement and locality constraints; they never show up in the completely random Lindbladians considered in Ref. [72].

Heuristically, this behavior matches our general picture [cf. Eq. (14)] that as steady-state entanglement increases, we have the emergence of an almost-conserved quantity, the projector onto the steady state. This separates the Hilbert space into two subspaces. One naively expects fast dynamics within each of these subspaces, with a single slow rate corresponding to mixing between the subspaces (for more details, see Appendix C). This picture matches the results of our numerics. One can picture the steady state and midgap state(s) as forming a quasistable slowly relaxing "slow manifold," whereas the rapidly decaying modes above the bulk gap are an effective "fast manifold." One could imagine tracing out the rapidly decaying states above the bulk gap to understand the slow dynamics within the midgap states(s) (see, e.g., Ref. [73]). It is especially interesting to note, though, that in this case the slow manifold contains only a handful of modes, whereas the fast manifold is growing exponentially with N.

B. Prethermalization and local relaxation

Given this hierarchy of relaxation rates, it is interesting to ask what kind of observables relax slowly via the midgap state and which relax quickly. Previous work on specific nonrandom models suggests that observables local to one subsystem tend to relax on fast $\mathcal{O}(\overline{\kappa})$ time scales, whereas nonlocal intersystem correlations relax slowly (see, e.g., Ref. [36]).

In order to study this, we want a system where we can independently look at the relaxation rate of the full A-B system, as well as trace out one subsystem and look
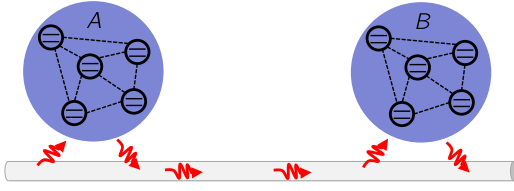
FIG. 3. A schematic showing two systems, A and B, that are coupled via a Markovian chiral (i.e., directional) waveguide, thus realizing a cascaded quantum system. The A system is "upstream" and its dynamics are unaffected by B (whereas B is indeed affected by A).

at the spectra of the other subsystem, which controls local observables. This can be achieved by constructing a unidirectional or cascaded [74–76] quantum system following the so-called "coherent quantum absorber" (CQA) approach [21] (see Fig. 3). Such a system still has the basic structure of our generic setup, where dissipative interactions between A and B are generated from local couplings to a common bath. Now, however, these interactions are directional: A influences B but not vice versa.

To achieve this directionality and still have the dynamics stabilize a chosen pure entangled steady state, we choose the matrices A_μ [cf. Eq. (24)] in each jump operator so that they obey the constraint equation

$$A_\mu = \Psi A_\mu^T \Psi^{-1}, \qquad (32)$$

where Ψ is defined via the steady state as per Eq. (23). This condition corresponds to imposing an effective classical detailed-balance condition (see Appendix D). We also add a Hamiltonian to our system $\hat{H}_{\mathrm{CQA}}$ that combines with each dissipator to enforce directionality (see Appendix D). Note that, previously, we have used Eq. (24) to define a dissipator given an arbitrary matrix A_μ; now, Eq. (32) also gives a constraint on which A_μ are allowed. Using both Eqs. (24) and (32) also tells us that $A_\mu = -B_\mu$, thus determining the form of each jump operator. Using this construction, we find that the dynamics of system A are given by

$$\mathrm{tr}_B[\partial_t \hat{\rho}] = \mathrm{tr}_B\left[-i[\hat{H}_{\mathrm{CQA}}, \hat{\rho}] + \sum_\mu \mathcal{D}[\hat{A}_\mu + \hat{B}_\mu]\hat{\rho} \right]$$

$$= -i[\hat{H}_A, \hat{\rho}_A] + \sum_\mu \mathcal{D}[\hat{A}_\mu]\hat{\rho}_A \equiv \hat{\mathcal{L}}_A \hat{\rho}_A, \quad (33)$$

where $\hat{\rho}_A \equiv \mathrm{tr}_B \hat{\rho}$. It thus follows that every eigenvalue of the system A Lindbladian $\hat{\mathcal{L}}_A$ is also an eigenvalue of the full Lindbladian $\hat{\mathcal{L}}$. Moreover, all observables on the A system relax according to the spectrum of $\hat{\mathcal{L}}_A$, whereas correlations between the two systems relax on a time scale governed by the gap of $\hat{\mathcal{L}}$. Note that because of Eq. (32), the Lindbladian $\hat{\mathcal{L}}_A$ necessarily satisfies classical detailed
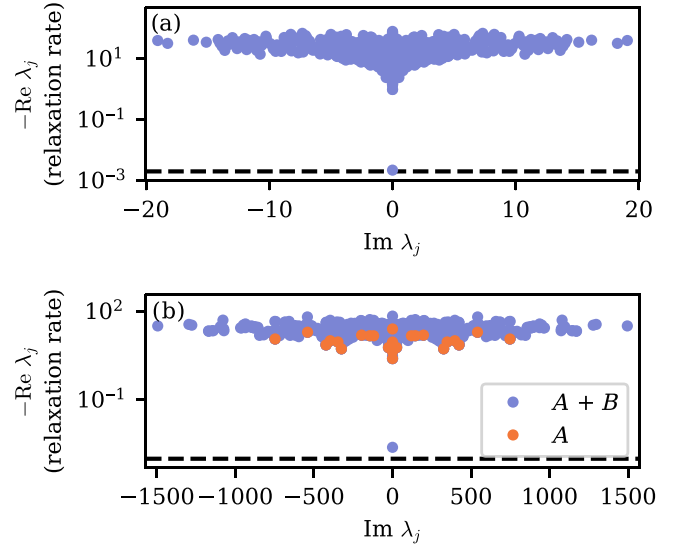

FIG. 4. (a) The spectrum of a realization of a random Lindbladian on a bipartite system, using the construction of Sec. IV A. Each random complex jump operator is constructed by drawing the matrix A_μ from the complex Ginibre ensemble with variance σ; this then determines B_μ via Eq. (24). (b) The spectrum of a realization of a random Lindbladian constructed using the CQA approach so that the interaction between A and B is necessarily directional [see Fig. 3 and Eq. (32)]. The blue points show the spectrum of the full Lindbladian $\hat{\mathcal{L}}$ and the orange points of the Lindbladian $\hat{\mathcal{L}}_A$ describe system-A-only dynamics. When looking at $\hat{\mathcal{L}}_A$ alone, there is no emergent slow mode and the dissipative gap is large. In both (a) and (b), the local dimension $N = 5$, there are $M = 2$ independent jump operators, and there is a pure random steady state with fixed $\delta\mathcal{E}_2 \equiv 10^{-3}$ [cf. Eq. (25)]. In both (a) and (b), the black dashed line shows $2(M-1)\sigma^2\delta\mathcal{E}_2$ [cf. Eq. (26)] and the steady state ($\lambda_0 = 0$) is not shown.

balance [also known as Gelfand-Naimark-Segal (GNS) detailed balance] [58,77].

In Fig. 4(b), we numerically sample a random distribution of Schmidt coefficients $\{p_i\}$ and constrain A_μ to obey the detailed balance condition given in Eq. (32). We also add the requisite Hamiltonian, making the system completely directional. Numerically, we observe that the full Lindbladian acting on both A and B has a small dissipative gap $\Delta \sim \overline{\kappa}\delta\mathcal{E}_2$, as predicted by the bound and consistent with a random jump operator as in Fig. 4(a). However, if we instead consider the spectrum of $\hat{\mathcal{L}}_A$, the Lindbladian of system A alone [cf. Fig. 3], the dissipative spectrum exhibits a large dissipative gap $\Delta \sim \overline{\kappa}$. This is in line with the results of Ref. [77], which studies the spectral properties of random Lindbladians satisfying classical (GNS) detailed balance. This separates the dynamics into two regimes. The first is a "prethermal" regime characterized by the $\mathcal{O}(\overline{\kappa})$ bulk gap; during this time, local observables can relax to their steady-state values as evidenced by the upstream system not experiencing slow-down. However,

intersystem correlations and entanglement approach their steady-state values on exponentially longer time scales, characterized by the true dissipative gap (see Fig. 4). This is in line with previously observed open-system dynamics with highly entangled steady states (that are not necessarily directional) (see, e.g., Ref. [36]).

C. Multiple slow modes

Our discussion of Lindbladian spectra has so far focused on cases in which, apart from our constraints on locality and having a pure entangled steady state, the dynamics are essentially unstructured. The slow-down of dynamics associated with increasing entanglement in this case can be attributed to the emergence of a single slow mode. We now ask how this situation is modified when our Lindbladian has some additional structure. We find regimes where now multiple slow modes (midgap states) arise due to increasing steady-state entanglement.

Consider the case in which we also have a notion of spatial locality *within* both the A and B subsystems. For example, consider two n-qubit spin chains denoted A and B, with local *XXZ* Hamiltonians governed by the master equation $\partial_t \hat{\rho} = -i[\hat{H}_{XXZ}, \hat{\rho}] + \hat{\mathcal{L}}_{\text{diss}}$, with

$$\hat{H}_{XXZ} = \sum_{s=A,B} \sum_{i=1}^{n-1} J\left(\hat{\sigma}_{s,i}^+ \hat{\sigma}_{s,i+1}^- + \text{H.c.}\right)$$
$$+ \sum_{s=A,B} \text{sgn}(s) \sum_{i=1}^{n-1} J_z \hat{\sigma}_{s,i}^z \hat{\sigma}_{s,i+1}^z, \quad (34)$$

$$\hat{\mathcal{L}}_{\text{diss}} = \mathcal{D}[u\hat{\sigma}_{A,1}^- + v\hat{\sigma}_{B,1}^+] + \mathcal{D}[u\hat{\sigma}_{B,1}^- + v\hat{\sigma}_{A,1}^+]. \quad (35)$$

Here, we take $\text{sgn}(A) = -\text{sgn}(B) = 1$ and $u^2 + v^2 = 1$. This models two spin chains being driven by two-mode squeezed-vacuum light at their boundary and in the limit $J_z = 0$ it has been considered as a method of entanglement generation [22,31,32,36]. This system has a pure steady state and thus is an example of the general class of dynamics [cf. Eqs. (4)–(6)] that we consider. The steady state can be found exactly (for related models, see Refs. [32,36]) and is independent of J, J_z:

$$|\psi\rangle_{\text{ss}} = \bigotimes_{i=1}^{n} \left[\sqrt{1-v^2}|0\rangle_{A,i}|0\rangle_{B,i} + (-1)^i v |1\rangle_{A,i}|1\rangle_{B,i}\right]. \quad (36)$$

It follows that the steady-state entanglement is controlled by v.

This system is clearly more structured than the completely random examples studied in the previous subsections. As such, one might expect that the Lindbladian spectrum would be very different, with potentially many more slow modes emerging when the steady state has high
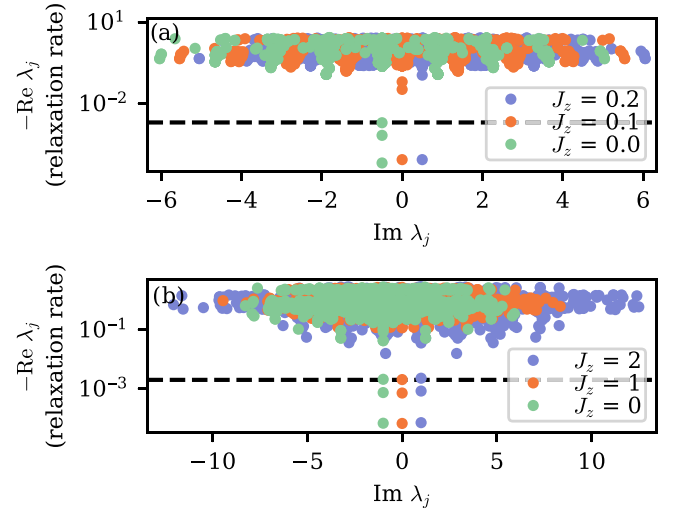

FIG. 5. (a) Lindbladian spectra for the master equation for two $n = 3$ qubit spin chains given by the *XXZ* Hamiltonian in Eq. (34) and the local boundary dissipation in Eq. (35) for varying values of the intrachain *ZZ* interaction J_z, with $J = 1$. Note that whenever $J_z > 0$ (and the Hamiltonian is no longer mappable to free fermions), all but one of the midgap states move into the bulk spectra. (b) Lindbladian spectra for the master equation for two $n = 3$ qubit spin chains given by $\hat{H} = \hat{H}_\parallel + \hat{H}_\perp$ [cf. Eqs. (37) and (38)] and the local boundary dissipation in Eq. (35) for varying values of the interchain *ZZ* interaction J_z. Note that this Hamiltonian always supports ballistic dynamics and that the slow modes are robust to interactions. In both (a) and (b), the steady-state entanglement is fixed to be $\delta \mathcal{E}_2 = 10^{-3}$ and the black dashed line is at $2(M-1)\delta \mathcal{E}_2$. Different values of J_z are offset horizontally to avoid overlap.

entanglement. Surprisingly, for generic parameters this is not the case (see Fig. 5): one still obtains a single slow mode.

However, for the special case in which $J_z = 0$, the situation is very different. For this parameter choice, the local Hamiltonian given in Eq. (34) is equivalent to a free-fermion Hamiltonian and we find the emergence of *multiple* slow modes for strong entanglement (see Fig. 5). Note that while the Hamiltonian alone can be mapped to noninteracting particles, the full dissipative dynamics still correspond to an interacting fermionic problem (for more details, see Ref. [36]). As such, it is surprising at first glance that the noninteracting nature of the Hamiltonian alone leads to such differences in the dissipative spectrum. Moreover, we observe numerically that the number of slow modes is exactly equivalent to n, the number of qubits in each chain, and hence is extensive in system size.

To see that the free-fermion dynamics are truly the cause of having multiple slow modes, we can consider a more complicated local Hamiltonian introduced in Ref. [78], which exhibits both free-fermion sectors of the Hilbert space, as well as diffusive sectors (see Appendix E). Specifically, consider the master equation

$\partial_t \hat{\rho} = -i[\hat{H}, \hat{\rho}] + \hat{\mathcal{L}}_{\text{diss}}$ with $\hat{\mathcal{L}}_{\text{diss}}$ defined as in Eq. (35) and $\hat{H} = \hat{H}_\parallel + \hat{H}_\perp$, with

$$\hat{H}_\parallel = J \sum_{i=1}^{n-1} \sum_{s=A,B} \hat{\sigma}_{s,i}^+ \hat{\sigma}_{s,i+1}^- + \text{H.c.,} \tag{37}$$

$$\hat{H}_\perp = \sum_{i=1}^{n} J \left(\hat{\sigma}_{A,i}^x \hat{\sigma}_{B,i}^x + \hat{\sigma}_{A,i}^y \hat{\sigma}_{B,i}^y \right) + J_z \hat{\sigma}_{A,i}^z \hat{\sigma}_{B,i}^z. \tag{38}$$

Here, $\hat{H}_\parallel$ is equivalent to the *XXZ* Hamiltonian in Eq. (34) at the free-fermion point $J_z = 0$. $\hat{H}_\perp$ couples the two chains together to form a two-rung ladder. Recall that a direct Hamiltonian coupling between subsystems A and B is allowed by our general locality constraint and does not impact the validity of our time-entanglement bounds. One can again show that the steady state is pure and is given by Eq. (36). Moreover, by plotting the dissipative spectra, we observe that there are still n slow modes separate from the bulk spectra, just as in the completely free case (see Fig. 5).

VI. CONCLUSIONS

In this paper, we have established a set of relations between pure steady-state entanglement and relaxation dynamics for a class of many-body open quantum systems, where two systems A and B have locality-constrained dissipative interactions (i.e., all dissipators are sums of local operators). We find that such a system can never have a unique maximally entangled steady state. Further, we have demonstrated that this result is a special case of a more general bound, which says that the time to reach the steady state is bounded below by how close that state is to being maximally entangled.

We have further explored this bound in the context of random Lindbladians satisfying our constraints, demonstrating that our bound accurately predicts the scaling of the dissipative gap with the steady-state entanglement. We have also considered the Lindbladian spectra of such models, finding that for large entanglement, they generically have a bulk gap accompanied by extremely slow midgap state(s), the number of which we conjecture is related to whether or not the Hamiltonian is mappable to free fermions.

We believe that these results provide new insights into dissipative entanglement generation. They are directly relevant to quantum reservoir engineering schemes targeting remote entanglement and they help to explain a number of previous results that have observed a trade-off between entanglement and preparation time in various specific systems. In future work, it would be interesting to explore further whether such entanglement-time constraints also apply to more general situations (e.g., extended many-body systems where one could try to connect entanglement

and relaxation times for different choices of regions A and B).

APPENDIX A: BOUND PROOF

1. Trace relation of maximally entangled states

Here, we will prove the trace property of maximally entangled states mentioned in the main text. Namely, if we define

$$|\psi\rangle = \frac{1}{\sqrt{N}} \sum_{i=1}^{N} |i\rangle_A \otimes |i\rangle_B, \tag{A1}$$

then, for any local operator $\hat{O}_A \otimes \mathbb{1}$, we can see that

$$\langle \psi | \hat{O}_A \otimes \mathbb{1} | \psi \rangle = \frac{1}{N} \sum_{i,j} \langle i | \hat{O}_A | j \rangle \otimes \langle i | j \rangle$$

$$= \frac{1}{N} \sum_i \langle i | \hat{O}_A | i \rangle = \frac{1}{N} \text{tr} \hat{O}_A. \tag{A2}$$

By the symmetry of the state under $A \leftrightarrow B$, this also tells us that the expectation value of any local B operator of the form $\mathbb{1} \otimes \hat{O}_B$ is also equivalent to its trace. Since for any jump operator $\hat{L} = \hat{A} \otimes \mathbb{1} + \mathbb{1} \otimes \hat{B}$ that is a sum of local operators, its commutator with its adjoint is also a sum of local operators,

$$[\hat{L}, \hat{L}^\dagger] = [\hat{A}, \hat{A}^\dagger] \otimes \mathbb{1} + \mathbb{1} \otimes [\hat{B}, \hat{B}^\dagger], \tag{A3}$$

then the expectation value

$$\langle \psi | [\hat{L}, \hat{L}^\dagger] | \psi \rangle = \frac{1}{N} \left(\text{tr}[\hat{A}, \hat{A}^\dagger] + \text{tr}[\hat{B}, \hat{B}^\dagger] \right) = 0, \tag{A4}$$

as noted in the main text.

2. Proof of main bound

We can now move on to proving the main bound. Following a similar construction to Ref. [79], we will bound

the fidelity to the steady state

$$F(t) = \left(\text{tr} \sqrt{\sqrt{\hat{\rho}_{\text{ss}}} \hat{\rho}_t \sqrt{\hat{\rho}_{\text{ss}}}} \right)^2. \qquad \text{(A5)}$$

Because we assume that the steady state is pure, this can be simplified as

$$F(t) = \text{tr}(\hat{\rho}_t \hat{\rho}_{\text{ss}}). \qquad \text{(A6)}$$

Now, we can bound the change in the fidelity by its maximal derivative, i.e.,

$$|F(t) - F(0)| \leq \Gamma_{\text{max}} t, \qquad \text{(A7)}$$

$$\Gamma_{\text{max}} = \max |\partial_t F(t)|, \qquad \text{(A8)}$$

and so we will now focus on bounding $\partial_t F(t)$. Letting $\hat{\mathcal{L}}$ be the Lindbladian and noting that $\hat{\rho}_{\text{ss}}$ is time independent,

we can observe that

$$|\partial_t F(t)| = |\text{tr}(\hat{\rho}_{\text{ss}} \partial_t \hat{\rho}_t)| = |\text{tr}(\hat{\rho}_{\text{ss}} \hat{\mathcal{L}} \hat{\rho}_t)|$$

$$= |\text{tr}(\hat{\mathcal{L}}^\dagger \hat{\rho}_{\text{ss}} \hat{\rho}_t)|, \qquad \text{(A9)}$$

where we have used the definition of the adjoint Lindbladian to move it onto steady state (where the adjoint is with respect to the Hilbert-Schmidt norm). The Cauchy-Schwartz inequality gives

$$\Gamma_{\text{max}} \leq |\text{tr}(\hat{\mathcal{L}}^\dagger \hat{\rho}_{\text{ss}} \hat{\rho}_t)| \leq \sqrt{\text{tr}(\hat{\mathcal{L}}^\dagger \hat{\rho}_{\text{ss}})^2 \text{tr}(\hat{\rho}_t)^2}$$

$$\leq \sqrt{\text{tr}(\hat{\mathcal{L}}^\dagger \hat{\rho}_{\text{ss}})^2}. \qquad \text{(A10)}$$

Thus the rate Γ_{max} is bounded by the Hilbert-Schmidt norm of the adjoint Lindbladian acting on the steady state. We can further simplify this as follows:

$$\hat{\mathcal{L}}^\dagger \hat{\rho}_{\text{ss}} = i[\hat{H}, \hat{\rho}_{\text{ss}}] + \sum_\mu \hat{L}_\mu^\dagger \hat{\rho}_{\text{ss}} \hat{L}_\mu - \frac{1}{2} \{\hat{L}_\mu^\dagger \hat{L}_\mu, \hat{\rho}_{\text{ss}}\}$$

$$= \sum_\mu \hat{L}_\mu^\dagger \hat{\rho}_{\text{ss}} \hat{L}_\mu \qquad \text{(A11)}$$

$$\implies \text{tr}(\hat{\mathcal{L}}^\dagger \hat{\rho}_{\text{ss}})^2 = \text{tr}\left[\sum_{\mu,\nu} \hat{L}_\mu^\dagger \hat{\rho}_{\text{ss}} \hat{L}_\mu \hat{L}_\nu^\dagger \hat{\rho}_{\text{ss}} \hat{L}_\nu \right]$$

$$= \sum_{\mu,\nu} |\langle \psi | [\hat{L}_\mu, \hat{L}_\nu^\dagger] | \psi \rangle|^2, \qquad \text{(A12)}$$

where we have repeatedly used the fact that $[\hat{H}, \hat{\rho}_{\text{ss}}] = \hat{L}_\mu \hat{\rho}_{\text{ss}} = 0$. Next, we will expand out the jump operator in terms of its matrix elements in the Schmidt basis:

$$\hat{L}_\mu = \hat{A}_\mu \otimes \mathbb{1} + \mathbb{1} \otimes \hat{B}_\mu$$

$$\equiv \sum_{ij}^N (A_\mu)_{ij} |i\rangle \langle j| \otimes \mathbb{1} + \mathbb{1} \otimes (B_\mu)_{ij} |i\rangle \langle j|. \qquad \text{(A13)}$$

To proceed, we will need to understand the relation between $(A_\mu)_{ij}$ and $(B_\mu)_{ij}$, which is implied by $\hat{L}_\mu |\psi\rangle = 0$. We find that, writing $|\psi\rangle$ in the Schmidt basis (and removing tensor-product signs for brevity),

$$0 = \sum_{ijkl}^N \sqrt{p_l} \left[(A_\mu)_{ij} |ik\rangle \langle jk| + (B_\mu)_{ij} |ki\rangle \langle kj| \right] |ll\rangle$$

$$= \sum_{ij}^N \left[\sqrt{p_j} (A_\mu)_{ij} + \sqrt{p_i} (B_\mu)_{ji} \right] |ij\rangle \qquad \text{(A14)}$$

$$\implies (A_\mu)_{ij} = -\sqrt{p_i} (B_\mu)_{ji} \frac{1}{\sqrt{p_j}}. \qquad \text{(A15)}$$

Recalling the definition of Ψ in Eq. (23), this is equivalent to

$$A_\mu = -\Psi B_\mu^T \Psi^{-1}, \tag{A16}$$

as stated in the main text [Eq. (24)]. Coming back to the bound, we can expand Eq. (A12) in terms of matrix elements as

$$\Gamma_{\max}^2 \leq \sum_{\mu,\nu} \left[\sum_{j,k=1}^N \left((A_\mu)_{j,k}(A_\nu)_{j,k}^* + (B_\mu)_{j,k}(B_\nu)_{j,k}^* \right) (p_j - p_k) \right]^2 \tag{A17a}$$

$$= \sum_{\mu,\nu} \left[\sum_{j,k=1}^N (A_\mu)_{j,k}(A_\nu)_{j,k}^* \frac{(p_j - p_k)^2}{p_k} \right]^2 \leq \sum_{\mu,\nu} \left[\frac{|A_\mu||A_\nu|}{p_{\min}} \sum_{j,k=1}^N (p_j - p_k)^2 \right]^2 \tag{A17b}$$

$$= \frac{1}{p_{\min}^2} \left(\sum_\mu |A_\mu|^2 \right)^2 \left[\sum_{j,k=1}^N (p_j - p_k)^2 \right]^2 = \frac{2N^2}{p_{\min}^2} \left(\sum_\mu |A_\mu|^2 \right)^2 \left(e^{-S^{(2)}} - N^{-1} \right)^2. \tag{A17c}$$

In Eq. (A17b), we have defined $|A_\mu|$ to be the largest matrix element of A_μ in the Schmidt basis and $\sqrt{p_{\min}}$ to be the smallest Schmidt coefficient. Taking a square root of both sides gives

$$\Gamma_{\max} \leq \frac{\sqrt{2}N}{p_{\min}} \left(\sum_\mu |A_\mu|^2 \right) \left(e^{-S^{(2)}} - N^{-1} \right), \tag{A18}$$

recovering the result from the main text.

3. Non-full-rank steady state

If Ψ is not full rank, then $p_{\min}^{-1}$ is ill defined. However, a similar bound can be derived for a state that is not full rank. Beginning at Eq. (A17), we note that

$$\Gamma_{\max}^2 \leq \sum_{\mu,\nu} \left[\sum_{j,k=1}^N \left((A_\mu)_{j,k}(A_\nu)_{j,k}^* + (B_\mu)_{j,k}(B_\nu)_{j,k}^* \right) (|\psi_j|^2 - |\psi_k|^2) \right]^2$$

$$\leq \sum_{\mu,\nu} \left(|A_\mu||A_\nu| + |B_\mu||B_\nu| \right)^2 \left[\sum_{j,k=1}^N \left| |\psi_j|^2 - |\psi_k|^2 \right| \right]^2$$

$$\leq N^2 \sum_{\mu,\nu} \left(|A_\mu||A_\nu| + |B_\mu||B_\nu| \right)^2 \sum_{j,k=1}^N (|\psi_j|^2 - |\psi_k|^2)^2$$

$$= 2N^3 \sum_{\mu,\nu} \left(|A_\mu||A_\nu| + |B_\mu||B_\nu| \right)^2 \left(e^{-S^{(2)}} - N^{-1} \right), \tag{A19}$$

$$\implies \quad \Gamma_{\max} \leq 2N^{3/2} \sqrt{\sum_{\mu,\nu} \left(|A_\mu||A_\nu| + |B_\mu||B_\nu| \right)^2} \left(e^{-S^{(2)}} - N^{-1} \right)^{1/2}$$

$$\leq 2N^{3/2} \left[\left(\sum_{\mu=1}^M |A_\mu| \right)^2 + \left(\sum_{\mu=1}^M |B_\mu| \right)^2 \right] \delta\mathcal{E}_2^{1/2}, \tag{A20}$$

where we see that the bound depends only on the root of $\delta\mathcal{E}_2$, as opposed to linearly for the case of a full-rank system.

4. Necessity of multiple jump operators

We now prove the result from the main text, that the condition Eq. (24) implies that A and B are isospectral, necessitating multiple jump operators (or a Hamiltonian interaction) to obtain a unique steady state. Let us begin by assuming that the matrix A is diagonalizable. The relation $A = -\Psi B^T \Psi^{-1}$ tells us that if A is diagonalizable via $A = P^{-1}DP$, then $B^T = -(P\Psi)^{-1}D(P\Psi)$. Hence, B is also diagonalizable as

$$B = (P\Psi)^T(-D)((P\Psi)^T)^{-1}. \tag{A21}$$

Thus, we can work in the (nonorthonormal) basis of eigenvectors of A and B, so that

$$\hat{L} = \hat{D}_A \otimes \mathbb{1} - \mathbb{1} \otimes \hat{D}_B, \tag{A22}$$

and therefore every vector of the form $|\psi\rangle = |i\rangle_A \otimes |i\rangle_B$ is in the kernel of $\hat{L}$, where $|i\rangle_{A,B}$ are the eigenbases of A and B, respectively.

Alternatively, let us assume that A is not diagonalizable. In this case, we can find a basis where it is in Jordan normal form. Let us consider just a single Jordan block of the form

$$A = \begin{pmatrix} \lambda & 1 & 0 & 0 & \dots & 0 \\ 0 & \lambda & 1 & 0 & \dots & 0 \\ \vdots & \vdots & \vdots & \ddots & \dots & 0 \\ 0 & 0 & 0 & \dots & \lambda & 1 \\ 0 & 0 & 0 & \dots & 0 & \lambda \end{pmatrix}, \tag{A23}$$

of dimension $n \times n$. Now, we can rewrite this in the following way: A has a single eigenvector that we will denote as $|0\rangle$, such that $A|0\rangle = \lambda|0\rangle$. Then, we define that $A|m\rangle = \lambda|m\rangle + |m-1\rangle$ for $m > 0$. Now, since A and $-B^T$ are similar matrices, they have an identical Jordan normal form. Hence, we can define an identical basis for B such that $B|m\rangle = -\lambda|m\rangle - |m-1\rangle$ (for $m > 0$) and $B|0\rangle = \lambda|0\rangle$. Now, consider the set of states

$$|\phi_n\rangle = \sum_{m=0}^{n} |m\rangle \otimes |n-m\rangle. \tag{A24}$$

We can observe that $\hat{L}|\phi_n\rangle$ is

$$\hat{L}|\phi_n\rangle = (A \otimes \mathbb{1} + \mathbb{1} \otimes B) \sum_{m=0}^{n} |m\rangle \otimes |n-m\rangle$$

$$= \sum_{m=1}^{n} |m-1\rangle \otimes |n-m\rangle - \sum_{m=0}^{n-1} |m\rangle \otimes |n-m-1\rangle$$

$$= 0. \tag{A25}$$

Repeating this construction for each Jordan block implies that the dimension of the kernel of $\hat{L}$ is always at least

N. To lift this degeneracy of the Lindbladian, we need (at least) two jump operators such that $\ker \hat{L}_1 \cap \ker \hat{L}_2$ is spanned by the steady state $|\psi\rangle$, or a Hamiltonian interaction such that the intersection of the eigenvectors of the Hamiltonian and the kernel of $\hat{L}$ is spanned by the steady state $|\psi\rangle$.

In Appendix B, we will do this by choosing multiple random jump operators.

5. Uneven Hilbert-space dimension

Throughout the main text, we mainly limit the discussion to bipartite Hilbert spaces in which each subspace has an identical Hilbert-space dimension. Now, we wish to explore what happens when considering systems of uneven dimension; without loss of generality, we will assume that $\mathcal{H} = \mathcal{H}_A \otimes \mathcal{H}_B$ and

$$\dim(\mathcal{H}_A) \equiv N_A < N_B \equiv \dim(\mathcal{H}_B). \tag{A26}$$

Now, we can still define a pure steady state in terms of its Schmidt coefficients:

$$|\psi\rangle = \sum_{i=1}^{N_A} \sqrt{p_i}|i\rangle_A \otimes |i\rangle_B, \tag{A27}$$

where the p_i are real and positive. We define the remaining $(N_B - N_A)$-dimensional subspace of $\mathcal{H}_B$ as

$$\mathcal{H}'_B = \mathcal{H}_B \setminus \text{span}\{|i\rangle_B | i = 1, \dots, N_A\}, \tag{A28}$$

for which we will define the basis $\{|i\rangle_B | i = N_A + 1, \dots, N_B\}$. A maximally entangled state is still defined by a flat distribution of Schmidt coefficients, where $p_i = N_A^{-1}$. Taking $\hat{L} = \hat{A} \otimes \mathbb{1} + \mathbb{1} \otimes \hat{B}$ as before, we now calculate $|\hat{L}^\dagger|\psi\rangle|^2$ when the $\hat{B}$ is of larger rank than $\hat{A}$ and $|\psi\rangle$ is maximally entangled. We now find that

$$|\hat{L}^\dagger|\psi\rangle|^2 = \langle\psi|[\hat{L}, \hat{L}^\dagger]|\psi\rangle$$

$$= \langle\psi|[\hat{A}, \hat{A}^\dagger] \otimes \mathbb{1}|\psi\rangle + \langle\psi|\mathbb{1} \otimes [\hat{B}, \hat{B}^\dagger]|\psi\rangle$$

$$= \text{tr}[\hat{A}, \hat{A}^\dagger] + \frac{1}{N_A} \sum_{i=1}^{N_A} \langle i|[\hat{B}, \hat{B}^\dagger]|i\rangle$$

$$= \frac{1}{N_A} \sum_{i=1}^{N_A} \sum_{j=N_A+1}^{N_B} |B_{ij}|^2 - |B_{ji}|^2. \tag{A29}$$

The condition $\hat{L}|\psi\rangle = 0$ implies (see Fig. 6)

$$B_{ij} = \begin{cases} A_{ji}\dfrac{\psi_i}{\psi_j}, & i,j \leq N_A, \\ 0, & i > N_A, j \leq N_A, \end{cases} \tag{A30}$$

which allows us to reduce Eq. (A29) to simply

$$|\hat{L}^\dagger|\psi\rangle|^2 = \frac{1}{N_A} \sum_{i=1}^{N_A} \sum_{j=N_A+1}^{N_B} |B_{ij}|^2, \quad \text{(A31)}$$

which can now be nonzero; i.e., it is possible to generate a maximally entangled state if $N_B > N_A$, as has been noted in the case of a qubit and qutrit in Ref. [30]. Let us define the projection operator $\hat{\Pi}$ as

$$\hat{\Pi} = \sum_{j=N_A+1}^{N_B} |j\rangle\langle j|. \quad \text{(A32)}$$

Then, Eq. (A30) tells us that $\hat{\Pi}\hat{B}(\mathbb{1} - \hat{\Pi}) = 0$. However, we also know that to avoid slow-down, we require that $||(\mathbb{1} - \hat{\Pi})\hat{B}\hat{\Pi}|| \neq 0$, as otherwise we can just truncate the Hilbert space and recover the bound for $N_A = N_B$. In fact, we can rewrite the bound in this case as

$$\Gamma_{\max} \leq \frac{\sqrt{2}N}{p_{\min}} \left(\sum_\mu |A_\mu|^2 \right) \delta\mathcal{E}_2 + \sum_\mu ||(\mathbb{1} - \hat{\Pi})\hat{B}_\mu\hat{\Pi}||_2^2, \quad \text{(A33)}$$

where the norm $||\hat{O}||_2$ is the operator norm, defined as the largest singular value of $\hat{O}$. The first term is simply the standard one from before and the second is a measure of how much the dissipation is utilizing the extra Hilbert space available. The use of an uneven Hilbert-space dimension to circumvent slow-down was first considered in a qubit-qutrit system in Ref. [30]; however, it should also work perfectly well in the many-body case. This can be seen in Fig. 6, where we take $N_B = N_A + 1$ and take A from the random Ginibre ensemble. We then take the elements of $(\mathbb{1} - \Pi)B\Pi$ to be normally distributed with zero mean and variance σ_B. Finally, we define the projection superoperator:

$$\hat{\mathcal{P}} = \sum_{i,j=1}^{N_A} |\rho_{ij}\rangle\rangle\langle\langle\rho_{ij}|, \quad \text{(A34)}$$

$$\hat{\rho}_{ij} = |i\rangle\langle i|_A \otimes |j\rangle\langle j|_B. \quad \text{(A35)}$$

(As before, the double-bracket notation $|\rho_{ij}\rangle\rangle$ signifies a vectorized density matrix.) If $\hat{\mathcal{L}}$ is the Lindbladian acting on the enlarged Hilbert space ($N_B > N_A$), then we can define

$$\hat{\mathcal{L}}' = \hat{\mathcal{P}}\hat{\mathcal{L}}\hat{\mathcal{P}}, \quad \text{(A36)}$$

which gives the effective dynamics in the subspace of dimension N_A^4. If we look at the gap as a function of σ_B^2, we can see that when $\sigma_B \ll \delta\mathcal{E}_2$, then the gap is dominated
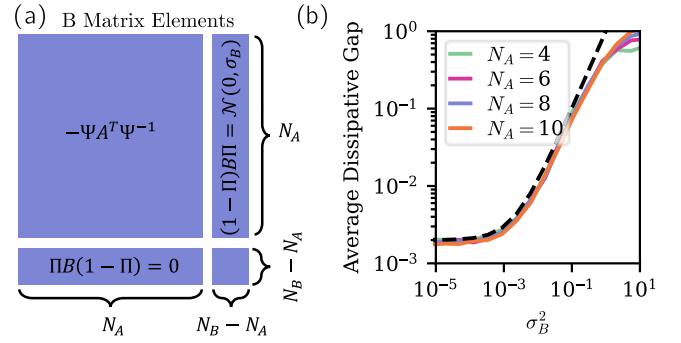

FIG. 6. (a) A depiction of the matrix elements of B when there is an uneven Hilbert-space dimension, breaking B into four blocks using the projector Π [cf. Eq. (A32)]. (b) The dissipative gap for random Lindbladians averaged over 100 instances, with $\delta\mathcal{E}_2$ fixed to be 10^{-3}. The A matrix is sampled from the random Ginibre ensemble with unit variance and the elements in $(\mathbb{1} - \Pi)B\Pi$ are sampled from a normal distribution with zero mean and variance σ_B^2. the elements of $(\mathbb{1} - \Pi)B(\mathbb{1} - \Pi)$ are irrelevant and taken to be 0. The black dashed line gives the expected scaling of $\sigma_B^2 + 2\delta\mathcal{E}_2$ until the gap saturates to an $\mathcal{O}(1)$ parameter for $\sigma_B^2 \gtrsim 1$.

by the entanglement-induced slow-down. However, when $\sigma_B^2 \gtrsim \delta S$, the gap opens up linearly in σ_B^2, before saturating at an $\mathcal{O}(1)$ value. Note that the projection $\hat{\mathcal{P}}$ is necessary, as otherwise when $\sigma_B^2 \ll 1$, the slow time scale would be dominated by the time to get out of the extra B system levels and we would not see the plateau at small σ_B^2.

An alternative interpretation is that systems on uneven Hilbert-space dimension can be recast as effectively being of equal dimension with non-full-rank steady-state Schmidt coefficients. That is to say, again assuming $N_B > N_A$, we can always define the operator

$$\tilde{A}_\mu = A_\mu \oplus 0_{N_B-N_A}, \quad \text{(A37)}$$

where by taking a direct sum with the 0 matrix, we essentially just pad A_μ with zeroes so that it is of the same dimension as B_μ. Next, we define the steady-state Schmidt coefficients

$$\tilde{\psi}_i = \left\{ \begin{array}{ll} \psi_i, & i \leq N_A, \\ 0, & N_A < i \leq N_B, \end{array} \right\} \quad \text{(A38)}$$

and again choose B_μ as in Eq. (A30). Now, we have a new master equation on an even Hilbert-space dimension with identical dynamics. We have simply augmented the Hilbert space with uncoupled extra levels on the A system. This means that the steady-state reduced density matrix is not full rank but the bound in Eq. (19) will still apply. Hence, given a state on an uneven Hilbert space, we can also state

that

$$\Gamma_{\max} \leq 2N_B^{3/2} \left[\left(\sum_{\mu=1}^{M} |A_\mu| \right)^2 + \left(\sum_{\mu=1}^{M} |B_\mu| \right)^2 \right]$$
$$\times \left(e^{-S_{ss}^{(2)}} - \frac{1}{N_B} \right)^{1/2}. \quad \text{(A39)}$$

In this case, $e^{-S_{ss}^{(2)}} \geq N_A^{-1}$ and so the gap will not close even for a maximally entangled state, as shown in, e.g., Ref. [30].

6. Mixing time

Another relevant quantity in both classical or quantum Markov chains is the mixing time [54], which can be thought of as the smallest time after which any initial probability distribution (or density matrix, in the quantum case) is within ϵ distance of the steady-state distribution. More formally, we can define this as

$$t_{\mathrm{mix}}(\epsilon) = \inf\{t > 0 \mid \forall \hat\rho, d_{\mathrm{tr}}(e^{\hat{\mathcal{L}}t}\hat\rho, \hat\rho_{\mathrm{ss}}) \leq \epsilon\}, \quad \text{(A40)}$$

where d_{tr} is the trace distance and $\hat\rho_{\mathrm{ss}}$ is the steady-state density matrix. The bound as stated in Eq. (18) is in terms of the quantum fidelity; however, this is related to the trace distance by [55]

$$d_{\mathrm{tr}}(\hat\rho, \hat\sigma) \geq 1 - F(\hat\rho, \hat\sigma), \quad \text{(A41)}$$

as long as at least one of $\hat\rho$ or $\hat\sigma$ is a pure state. Thus, if we now use that $F(e^{\hat{\mathcal{L}}t}\hat\rho, \hat\rho_{\mathrm{ss}}) \leq F(\hat\rho, \hat\rho_{\mathrm{ss}}) + vt$, then we find that

$$\epsilon \geq d_{\mathrm{tr}}(e^{\hat{\mathcal{L}}t}\hat\rho, \hat\rho_{\mathrm{ss}}) \geq 1 - F(e^{\hat{\mathcal{L}}t}\hat\rho, \hat\rho_{\mathrm{ss}})$$
$$\geq 1 - F(\hat\rho, \hat\rho_{\mathrm{ss}}) - \Gamma_{\max} t \quad \text{(A42)}$$
$$\implies \quad \Gamma_{\max} t \geq 1 - \epsilon - F(\hat\rho, \hat\rho_{\mathrm{ss}}) \quad \text{(A43)}$$
$$\implies \quad t_{\mathrm{mix}}(\epsilon) \geq \frac{1 - \epsilon}{\Gamma_{\max}} \quad \text{(A44)}$$

where $\Gamma_{\max}$ is bounded from above by Eq. (18) as derived before. Hence, the mixing time is lower bounded by one over the distance from the maximal entropy.

APPENDIX B: RANDOM LINDBLADIANS

1. Random jump operators

It is useful to consider how well the bound is saturated on a class of random Lindbladians, as shown in the main text. Let us define a distribution of Schmidt coefficients $\{p_i\}$ subject to

$$\sum_i p_i = 1, \quad -\log \sum_i p_i^2 = S^{(2)}, \quad \text{(B1)}$$

for some fixed value of the Renyi-2 entropy $S^{(2)}$. Now, given this distribution, we define a set of random matrices A_μ sampled from the complex Ginibre ensemble where $(A_\mu)_{ij}$ are independent identically distributed (IID) Gaussian random variables with

$$\mathbb{E}[(A_\mu)_{ij}] = 0, \quad \mathbb{E}[(A_\mu)^*_{ij}(A_\nu)_{kl}] = \delta_{ik}\delta_{jl}\delta_{\mu\nu}\sigma^2. \quad \text{(B2)}$$

We will sample random jump operators from many ensembles, including the complex Ginibre ensemble, random Hermitian matrices, random symmetric matrices, and random matrices that obey detailed balance. For concreteness, let us define A drawn from the random Ginibre ensemble above [Eq. (B2)]. Then, we define the random Hermitian operator A_H, the random symmetric operator A_S, and the random detailed-balance operator A_{DB} as

$$A_H = \frac{1}{\sqrt{2}}(A + A^\dagger), \quad \text{(B3a)}$$

$$A_S = \frac{1}{\sqrt{2}}(A + A^T), \quad \text{(B3b)}$$

$$A_{DB} = \frac{1}{\sqrt{2}}(A_S + \Psi A_S^T \Psi^{-1}). \quad \text{(B3c)}$$

For all of these ensembles, we find that the dissipative gap scales linearly with $\delta\mathcal{E}_2$ predicted by the bound. This is shown in Fig. 7.

2. Fidelity rate of change from a Haar-random state

The bound given in Eq. (18) says that no state can approach the steady state at a rate faster than $\mathcal{O}(N^2) \times \delta\mathcal{E}_2$. However, the numerics seem to imply that the dissipative gap is actually $\mathcal{O}(1) \times \delta\mathcal{E}_2$. One might guess that this discrepancy is a result of the fact that the dissipative gap is the slowest-relaxing mode, whereas the bound applies to the fastest. To obtain a prefactor closer to $\mathcal{O}(1)$, we can consider bounding a Haar-random state as opposed to all states. Recalling the formula from above [Eq. (A9)], we know that

$$\partial_t F(t) = \mathrm{tr}\left(\hat\rho_t \hat{\mathcal{L}}^\dagger \hat\rho_{\mathrm{ss}} \right). \quad \text{(B4)}$$

Let $\hat\rho_t = \hat{U}|0\rangle\langle 0|\hat{U}^\dagger$, with $\hat{U}$ integrated over the Haar measure. Since $\partial_t F(t)$ is linear in $\hat\rho_t$, we can just directly
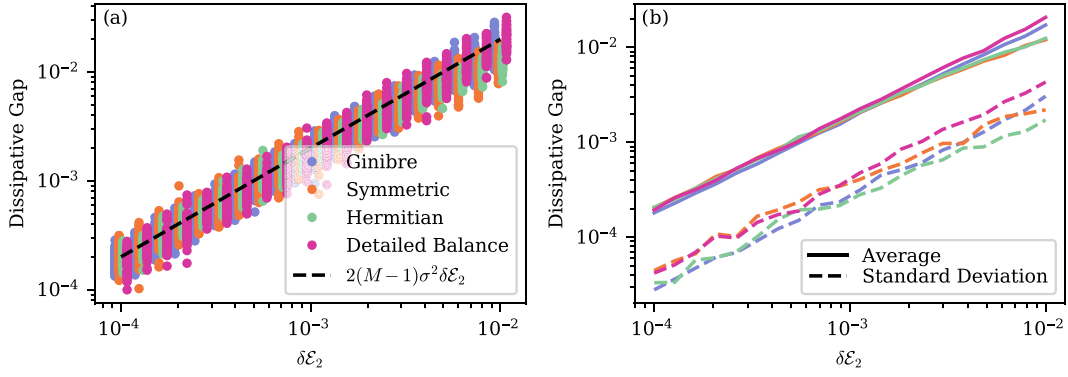
FIG. 7. (a) The dissipative gap of the random Lindbladians given a fixed steady-state entanglement $\mathcal{E}_2$, similar to Fig. 2. The different colors correspond to drawing the matrix A from different distributions (see Eq. (B3)). For each distribution and entanglement value, we sample 100 Lindbladians, with local dimension $N = 10$ and $M = 2$ jump operators. The black dashed line gives the scaling as predicted in Eq. (27). (b) The average (solid lines) and standard deviation (dashed lines) of the points in (a) for a fixed value of entanglement and distribution.

calculate that

$$\int_{\text{Haar}} \hat{U}|0\rangle\langle 0|\hat{U}^\dagger \, dU = \frac{\mathbb{1}}{N^2} \tag{B5}$$

$$\implies \int_{\text{Haar}} \partial_t F(t) \, dU = \frac{1}{N^2} \text{tr}\left(\hat{\mathcal{L}}^\dagger \hat{\rho}_{\text{ss}}\right). \tag{B6}$$

Now, we can calculate that

$$\frac{1}{N^2}\text{tr}\left(\hat{\mathcal{L}}^\dagger \hat{\rho}_{\text{ss}}\right) = \frac{1}{N^2}\sum_\mu \langle \psi | [\hat{L}_\mu, \hat{L}_\mu^\dagger] | \psi \rangle$$

$$= \frac{1}{N^2}\sum_\mu \sum_{j,k=1}^N |(A_\mu)_{j,k}|^2 \frac{(p_j - p_k)^2}{p_k}. \tag{B7}$$

Now, at this point, we can see that this can be bounded in a similar way as before by

$$\int_{\text{Haar}} \partial_t F(t) \, dU \le \left(\sum_\mu |A_\mu|^2\right)\frac{2}{N p_{\text{min}}}\delta\mathcal{E}_2. \tag{B8}$$

We can be more precise if we know something about the distributions from which we sample A_μ and p_j. Suppose that (A_μ) is sampled from a random distribution with variance

$$\mathbb{E}\left[|(A_\mu)_{j,k}|^2\right] = \sigma^2. \tag{B9}$$

Further, let us rewrite the Schmidt coefficients in the following, physically motivated, form:

$$p_i = \frac{e^{-\beta\lambda_i}}{\sum_{j=1}^N e^{-\beta\lambda_j}}, \tag{B10}$$

where we have defined a new set of random variables λ_i. Note that by writing it in this manner, the fact that

$\sum_{i=1}^N p_i = 1$ is inherently manifest. Moreover, we have a single parameter β that can tune the steady-state entanglement entropy. When $\beta = 0$, then $p_i = 1/N$ and the state is maximally entangled. As $\beta \to \infty$, the state becomes pure. Moreover, $\delta\mathcal{E}_2(\beta)$ is monotonic in β, so there is a unique value of β to fix the entanglement. Next, observe that if $\lambda_i \to \lambda_i - \bar{\lambda}$, then p_i are invariant, so without loss of generality we can take $\sum_{i=1}^N \mathbb{E}[\lambda_i] = 0$. Next, we will set a scale for β by defining

$$\frac{1}{N}\sum_{i=1}^N \mathbb{E}[\lambda_i^2] = 1. \tag{B11}$$

We can always do this (for any distribution with a well-defined second moment) by rescaling β. Finally, we will define the variable $\chi^2 = \sum_{i,j=1}^N \mathbb{E}[\lambda_i\lambda_j]$. For example, if λ_i are IID, then $\chi^2 = N$. To calculate the average of the rate of change of the fidelity, it will be necessary to compute the average $\sum_{i=1}^N \mathbb{E}[p_i^{-1}]$. We can make progress by noting that in the high-entanglement limit, the variance of the p_i is highly constrained by fixing the entropy. Hence, we can compute this to leading order in $\delta\mathcal{E}_2$ (or equivalently, the small β limit). Observe that

$$\mathbb{E}[\delta\mathcal{E}_2] = \mathbb{E}\left[\frac{\sum_{i=1}^N e^{-2\beta\lambda_i}}{\left(\sum_{j=1}^N e^{-\beta\lambda_j}\right)^2}\right]$$

$$= \frac{\beta^2}{N}\left(1 - \frac{\chi^2}{N^2}\right) + \mathcal{O}(\beta^4 N^2). \tag{B12}$$

Now, $\delta\mathcal{E}_2$ is in fact fixed, so we can invert this to instead be an equation for β:

$$\frac{\beta^2}{N}\left(1 - \frac{\chi^2}{N^2}\right) = \delta\mathcal{E}_2 + \mathcal{O}(\delta\mathcal{E}_2 N^2)^2. \tag{B13}$$

From here, we can now calculate, to leading order in β,

$$
\sum_{i=1}^{N} \mathbb{E}[p_i^{-1}] = \sum_{i,j=1}^{N} \mathbb{E}\left[e^{-\beta(\lambda_i - \lambda_j)}\right]
$$

$$
= N^2 + \frac{\beta^2}{2} \sum_{j,k=1} \mathbb{E}\left[(\lambda_i - \lambda_j)^2\right] + \mathcal{O}(\beta^4 N^2)
$$

$$
= N^2 \left(1 + N\delta\mathcal{E}_2\right) + \mathcal{O}(N^2 \delta\mathcal{E}_2)^2. \tag{B14}
$$

We can use this relation to observe that Eq. (B7) simplifies to

$$
\mathbb{E}\left[\int_{\text{Haar}} \partial_t F(t) \, \mathrm{d}U\right] = \mathbb{E}\left[\frac{1}{N^2} \sum_{\mu=1}^{M} \sum_{j,k=1}^{N} |(A_\mu)_{j,k}|^2 \frac{(p_j - p_k)^2}{p_k}\right]
$$

$$
= \frac{M\sigma^2}{N^2} \mathbb{E}\left[\sum_{j,k=1}^{N} \frac{(p_j - p_k)^2}{p_k}\right]
$$

$$
= 2M\sigma^2 \delta\mathcal{E}_2 + \mathcal{O}(\delta\mathcal{E}_2)^2, \tag{B15}
$$

where we have defined M to be the number of jump operators. Assuming that $N\delta\mathcal{E}_2 \ll 1$, we can drop the second term as small and recover the result quoted in the main text. We can also calculate the variance that one would expect from such a distribution. Here, we calculate

$$
\mathbb{E}\left[\int_{\text{Haar}} |\partial_t F(t)|^2 \, \mathrm{d}U\right] = \mathbb{E}\left[\int_{\text{Haar}} \left|\sum_\mu |\langle\psi|L_\mu U|0\rangle|^2\right|^2 \mathrm{d}U\right]. \tag{B16}
$$

This now depends nonlinearly on $\hat\rho_t$, so we cannot simply replace the state with its average. However, we can still make progress. We will suppress the integral over the Haar measure for brevity, giving

$$
\mathbb{E}\left[|\partial_t F|^2\right] = \mathbb{E}\left[\left|\sum_\mu |\langle\psi|\hat{L}_\mu \hat{U}|0\rangle|^2\right|^2\right]
$$

$$
= \mathbb{E}\left[\sum_{i_\alpha j_\alpha}^{N} \sum_{\mu,\nu}^{m} (A_\mu)_{j_1 k_1} (A_\nu)_{j_2 k_2} (A_\mu)_{j_3 k_3}^* (A_\nu)_{j_4 k_4}^* U_{00}^{k_1 j_1} U_{00}^{k_2 j_2} (U_{00}^{k_3 j_3})^* (U_{00}^{k_4 j_4})^* \prod_\alpha \left(\sqrt{p_{j_\alpha}} - \frac{p_{k_\alpha}}{\sqrt{p_{j_\alpha}}}\right)\right]
$$

$$
= \sigma^4 \sum_{i_\alpha j_\alpha}^{N} \sum_{\mu,\nu}^{m} \left(\delta_{13}\delta_{24} + \delta_{14}\delta_{23}\delta_{\mu\nu}\right) \mathbb{E}\left[U_{00}^{k_1 j_1} U_{00}^{k_2 j_2} (U_{00}^{k_3 j_3})^* (U_{00}^{k_4 j_4})^* \prod_\alpha \left(\sqrt{p_{j_\alpha}} - \frac{p_{k_\alpha}}{\sqrt{p_{j_\alpha}}}\right)\right]
$$

$$
= \sigma^4 \sum_{i_\alpha j_\alpha}^{N} \left(M^2 \delta_{13}\delta_{24} + m\delta_{14}\delta_{23}\right) \frac{(\delta_{13}\delta_{24} + \delta_{14}\delta_{23})}{N^2(N^2+1)} \mathbb{E}\left[\prod_\alpha \left(\sqrt{p_{j_\alpha}} - \frac{p_{k_\alpha}}{\sqrt{p_{j_\alpha}}}\right)\right]
$$

$$
= \frac{\sigma^4(M^2 + M)}{N^2(N^2+1)} \sum_{i_\alpha j_\alpha}^{N} (\delta_{13}\delta_{24} + \delta_{1234}) \mathbb{E}\left[\prod_\alpha \left(\sqrt{p_{j_\alpha}} - \frac{p_{k_\alpha}}{\sqrt{p_{j_\alpha}}}\right)\right]
$$

$$
= \frac{\sigma^4(M^2 + M)}{N^2(N^2+1)} \mathbb{E}\left[\left(\sum_{jk}^{N} \frac{(p_j - p_k)^2}{p_j}\right)^2 + \sum_{jk}^{N} \frac{(p_j - p_k)^4}{p_j^2}\right]. \tag{B17}
$$

To make progress, we will again assume that $\delta\mathcal{E}_2 \ll N^{-2}$ and so we can again expand to leading order in $\delta\mathcal{E}_2 N^2$. We will also assume $N \gg 1$ and so we will only keep terms to leading order in N^{-1} as well. This gives

$$\mathbb{E}\left[|\partial_t F|^2\right] = \sigma^4(M^2 + M + \mathcal{O}(N^{-2}))\,(\delta\mathcal{E}_2)^2 \\ + \mathcal{O}(N^2 \delta\mathcal{E}_2)^3. \tag{B18}$$

This tells us that we would expect a variance of

$$\mathbb{V}\left[|\partial_t F|\right] = \mathbb{E}\left[|\partial_t F|^2\right] - |\mathbb{E}\left[|\partial_t F|\right]|^2 \\ = \sigma^4 M\,(\delta\mathcal{E}_2)^2 + \mathcal{O}(\delta\mathcal{E}_2)^3 \\ = \frac{1}{M}\,|\mathbb{E}\left[|\partial_t F|\right]|^2 + \mathcal{O}(\delta\mathcal{E}_2)^3 \tag{B19}$$

and so the distribution should get tighter as one adds more and more jump operators. This scaling can be observed in Fig. 8. However, we note that in Fig. 8 we are plotting the dissipative gap and not the rate of change of the fidelity. This is important because we know analytically that the gap $\Delta = 0$ if $M = 1$, given the fact that $\hat{A}$ and $\hat{B}$ are isospectral (see Sec. A 4). However, a single jump operator is sufficient to change the fidelity to the steady state at a nonzero rate for some states in the Hilbert space. Hence, we expect that the average and variance of the gap should be (setting $\sigma = 1$)

$$\mathbb{E}[\Delta] \propto (M-1)\delta\mathcal{E}_2, \tag{B20}$$

$$\mathbb{V}[\Delta] \propto (M-1)\,(\delta\mathcal{E}_2)^2. \tag{B21}$$

Hence, in Fig. 8 we normalize by these values and observe a collapse of both the average and the standard deviation (the root of the variance) onto a single line.

APPENDIX C: MAXIMALLY ENTANGLED STATE AS A STRONG SYMMETRY

Recall from Appendix A that if $\hat{\rho}_{ss}$ is a maximally entangled state, then $\hat{\rho}_{ss}\hat{L}_\mu = 0$. However, because to be a steady state requires $\hat{L}_\mu\hat{\rho}_{ss} = 0$, this implies that the commutator of the steady state with each jump operator identically vanishes. Additionally, any pure steady state must be a Hamiltonian eigenstate as well, so all together this implies that

$$[\hat{L}_\mu, \hat{\rho}_{ss}] = [\hat{H}, \hat{\rho}_{ss}] = 0. \tag{C1}$$

However, this is simply the statement that $\hat{\rho}_{ss}$ is a *strong symmetry* of the dynamics [53]. This means that we can interpret the steady-state density matrix as a symmetry operator; i.e., it is a conserved charge. Because it is a pure state, $\hat{\rho}_{ss} = |\psi\rangle\langle\psi|$, the density matrix is itself simply a projection operator onto the steady state $|\psi\rangle$ and so the
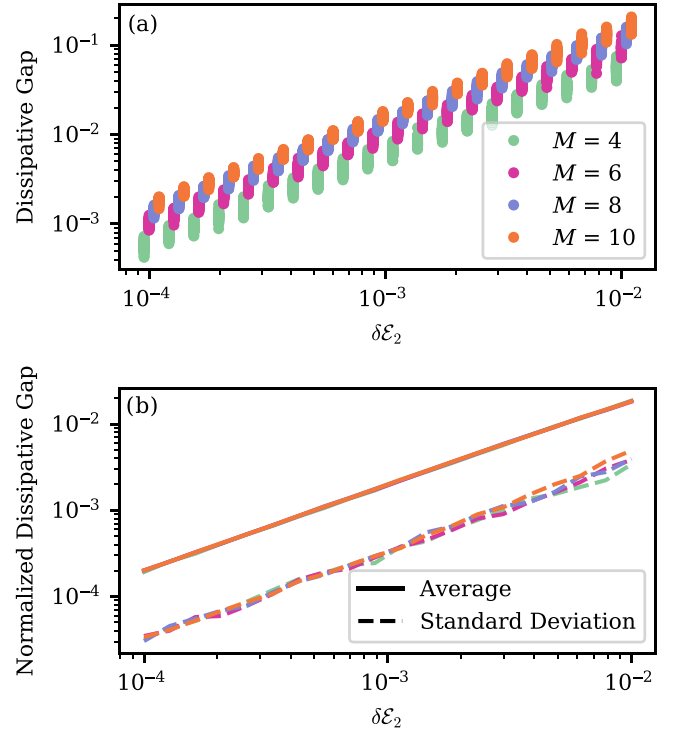

FIG. 8. (a) The dissipative gap of random Lindbladians, with A_μ sampled from the complex Ginibre ensemble and local dimension $N = 10$ for varying numbers of jump operators M. There are 100 samples for each M and each value of entanglement $\delta\mathcal{E}_2$. (b) The normalized average (solid lines) and standard deviation (dashed lines) of the data in (a). The average is normalized as $\mathbb{E}[\Delta]/(m-1)$ [cf. Eq. (B20)] and the standard deviation as $\sqrt{\mathbb{E}[\Delta^2] - \mathbb{E}[\Delta]^2/m - 1}$ [cf. Eq. (B21)].

conserved charge generated by such a symmetry is simply the population in the steady state. Hence, this is another way to see that if an open system has a steady state that is maximally entangled, then it is completely dynamically isolated from the rest of the system.

Now, let us suppose that we perturb the Lindbladian slightly away from this point, so that the steady state is still pure but slightly less entangled. In this case we still have that

$$\hat{L}_\mu\hat{\rho}_{ss} = [\hat{H}, \hat{\rho}_{ss}] = 0, \tag{C2}$$

since it is by definition a pure steady state, but if it is not maximally entangled, then generically $\hat{\rho}_{ss}\hat{L}_\mu \neq 0$. We can quantify, then, how close this is to being a symmetry by defining the error $\mathcal{E}$:

$$\mathcal{E} = \sum_\mu |[\hat{L}_\mu, \hat{\rho}_{ss}]| = \sum_\mu \langle\psi|[\hat{L}_\mu, \hat{L}_\mu^\dagger]|\psi\rangle = \text{tr}\left(\hat{\mathcal{L}}^\dagger\hat{\rho}_{ss}\right), \tag{C3}$$

where $|\cdot|$ denotes the Hilbert-Schmidt norm. However, this is exactly the same term that shows up when calculating the rate of change of the fidelity, which we know goes to zero as [cf. Eqs. (B7) and (B8)]

$$\sum_\mu \langle\psi|[\hat{L}_\mu, \hat{L}_\mu^\dagger]|\psi\rangle \lesssim N^2 \delta\mathcal{E}_2, \qquad \text{(C4)}$$

and so we can think of this entanglement term both as bounding how fast the fidelity to the steady state can change as well as how close the Lindbladian is to having a strong symmetry.

This interpretation also explains why there is exactly one midgap state for a random Lindbladian. Let us suppose that we have a Lindbladian $\hat{\mathcal{L}}_0$ with a maximally entangled steady state $\hat{\rho}_0 = |\psi_{\max}\rangle\langle\psi_{\max}|$. Now, we know that this implies that there is a strong symmetry in the dynamics and therefore at least twofold degeneracy in the steady-state manifold. Moreover, in the absence of any other symmetry constraints, the degeneracy should be exactly two and it should be split by a $\Delta_{\text{bulk}} = \mathcal{O}(1)$ bulk gap [72]. Now, let us assume that there is a very closely related Lindbladian $\hat{\mathcal{L}} = \hat{\mathcal{L}}_0 + \epsilon\hat{\mathcal{L}}_1$ such that $\epsilon \ll \Delta_{\text{bulk}}$ the bulk gap and so we can perform perturbation theory within the steady-state manifold.

Now, we do not know exactly what the degenerate steady state actually is but we do know exactly what the *left eigenvectors* are, so instead we will do perturbation theory in $\hat{\mathcal{L}}^\dagger$, which has the same eigenspectrum of $\hat{\mathcal{L}}$. Explicitly, we know that $\hat{\mathcal{L}}_0^\dagger\hat{\rho}_0 = \hat{\mathcal{L}}_0^\dagger(\mathbb{1} - \hat{\rho}_0) = 0$.

Let us suppose that $\hat{\rho}_{\text{ss}}$ is the unique steady-state solution of $\hat{\mathcal{L}}\hat{\rho}_{\text{ss}} = 0$. Then, $\hat{\rho}_{\text{ss}} = \hat{\rho}_0 + \epsilon\hat{\rho}_1 + \mathcal{O}(\epsilon^2)$. Therefore, $\hat{\rho}_0 = \hat{\rho}_{\text{ss}} + \mathcal{O}(\epsilon)$ and, specifically, this means that the left eigenvector of $\hat{\mathcal{L}}$—or, alternatively, the right eigenvector of $\hat{\mathcal{L}}^\dagger$—is $\hat{\rho}_0 + \mathcal{O}(\epsilon) = \hat{\rho}_{\text{ss}} + \mathcal{O}(\epsilon)$. Hence, to first order in ϵ, we can perturbatively calculate the steady-state degeneracy splitting as the eigenvalues of

$$\text{tr}\left[\begin{pmatrix} \mathbb{1} - \hat{\rho}_{\text{ss}} \\ \hat{\rho}_{\text{ss}} \end{pmatrix} \hat{\mathcal{L}}^\dagger \begin{pmatrix} \mathbb{1} - \hat{\rho}_{\text{ss}} & \hat{\rho}_{\text{ss}} \end{pmatrix}\right]$$

$$= \text{tr}\left[\begin{pmatrix} \mathbb{1} \\ 0 \end{pmatrix} \hat{\mathcal{L}}^\dagger \begin{pmatrix} -\hat{\rho}_{\text{ss}} & \hat{\rho}_{\text{ss}} \end{pmatrix}\right]$$

$$= \begin{pmatrix} -\Gamma & \Gamma \\ 0 & 0 \end{pmatrix}, \qquad \text{(C5)}$$

where $\Gamma = \text{tr}(\hat{\mathcal{L}}^\dagger\hat{\rho}_{\text{ss}})$. The eigenvalues of this matrix are $0, -\Gamma$, so perturbatively one would expect a dissipative gap that is equivalent to $\Gamma = \text{tr}(\hat{\mathcal{L}}^\dagger\hat{\rho}_{\text{ss}})$. However, this is just exactly the error $\mathcal{E}$ defined in Eq. (C3); i.e., the dissipative gap is equivalent to how close the system is to having a strong symmetry.

APPENDIX D: DIRECTIONAL DYNAMICS

As mentioned in the main text, the form of the jump operator given in Eq. (6) is the correct form for directional dynamics [21,74–76]. To achieve directionality, such that the dynamics in the A system are unaffected by those in the B system, a Hamiltonian interaction is necessary. Generically, given a jump operator $\hat{L} = \hat{A} \otimes \mathbb{1} + \mathbb{1} \otimes \hat{B}$, one can always make this a unidirectional (chiral) process via the Hamiltonian [21,76]

$$\hat{H}_{AB} = \frac{i}{2}\left(\hat{A}^\dagger\otimes\hat{B} - \hat{A}\otimes\hat{B}^\dagger\right). \qquad \text{(D1)}$$

More is needed, however, to ensure that the state we began with is still the steady state of this new Lindbladian.

To make this possible, first we will need a local Hamiltonian $\hat{H}_A$ on the A system such that

$$\hat{\mathcal{L}}_A\hat{\rho}_A = -i[\hat{H}_A, \hat{\rho}_A] + \mathcal{D}[\hat{A}]\hat{\rho}_A = 0, \qquad \text{(D2)}$$
$$\hat{\rho}_A \equiv \text{tr}_B\hat{\rho}_{\text{ss}}. \qquad \text{(D3)}$$

This is equivalent to the condition that

$$(H_A)_{nm} = \frac{i}{p_m - p_n}\langle n|\mathcal{D}[\hat{A}]\hat{\rho}_A|m\rangle, \qquad \text{(D4)}$$

which uniquely defines the matrix elements of H_A in the Schmidt basis. Note that this also gives another constraint, that

$$\langle n|\mathcal{D}[\hat{A}]\hat{\rho}_A|n\rangle = 0, \qquad \text{(D5)}$$
$$\implies \sum_k |A_{nk}|^2 p_k - |A_{kn}|^2 p_n = 0. \qquad \text{(D6)}$$

One way to satisfy this is to simply assume $A = \Psi A^T \Psi^{-1}$, which is what we have done throughout this paper.

With $\hat{H}_A$ now defined, we can use the general CQA construction in Ref. [21] to find the local Hamiltonian on B, which is given by

$$H_B = -\frac{1}{2}\Psi\left(H_A - \frac{i}{2}A^\dagger A\right)^T \Psi^{-1} + \text{H.c.} \qquad \text{(D7)}$$

Then, we can define

$$\hat{H}_{\text{CQA}} = \hat{H}_A \otimes \mathbb{1} + \mathbb{1} \otimes \hat{H}_B + \hat{H}_{AB}, \qquad \text{(D8)}$$
$$\hat{\mathcal{L}}_{\text{CQA}}\hat{\rho} = \mathcal{D}[\hat{A} \otimes \mathbb{1} + \mathbb{1} \otimes \hat{B}]\hat{\rho} - i[\hat{H}_{\text{CQA}}, \hat{\rho}], \qquad \text{(D9)}$$

which generates directional dynamics with the steady state $\hat{\rho}_{\text{ss}}$ as desired.

APPENDIX E: FREE-FERMION SUBSPACES OF AN INTERACTING HAMILTONIAN

In the main text, we consider the interacting two-leg ladder Hamiltonian $\hat{H} = \hat{H}_{\parallel} + \hat{H}_{\perp}$, where $\hat{H}_{\parallel}$ is an *XX* Hamiltonian running along the legs of the ladder and $\hat{H}_{\perp}$ is an anisotropic *XXZ* Hamiltonian across the rungs:

$$\hat{H}_{\parallel} = J \sum_{i=1}^{n-1} \sum_{s=A,B} \hat{\sigma}_{s,i}^{+} \hat{\sigma}_{s,i+1}^{-} + \text{H.c.}, \tag{E1a}$$

$$\hat{H}_{\perp} = \sum_{i=1}^{n} J\left(\hat{\sigma}_{A,i}^{x}\hat{\sigma}_{B,i}^{x} + \hat{\sigma}_{A,i}^{y}\hat{\sigma}_{B,i}^{y}\right) + J_z\hat{\sigma}_{A,i}^{z}\hat{\sigma}_{B,i}^{z}, \tag{E1b}$$

This Hamiltonian has been introduced in Ref. [78], where it has been shown that (see also Ref. [32]) the Hamiltonian can be recast as particles hopping on a 1D chain, where now each lattice site has local Hilbert-space dimension $d = 4$. Define the singlet and triplet states $|S/T\rangle_j$ as

$$|S/T\rangle_j = \frac{1}{\sqrt{2}}\left(|0\rangle_{A,j}|1\rangle_{B,j} \mp |1\rangle_{A,j}|0\rangle_{B,j}\right). \tag{E2}$$

Letting $|0\rangle_j \equiv |0\rangle_{A,j}|0\rangle_{B,j}$ and, similarly, $|1\rangle_j \equiv |1\rangle_{A,j}|1\rangle_{B,j}$, then $\{|0\rangle, |1\rangle, |S\rangle, |T\rangle\}$ span the local Hilbert space of the single 1D chain.

Next, it is simple to observe that because the *XXZ* interaction conserves total angular momentum as well as total *Z* angular momentum on each bond, then these four states can also be used to form an eigenbasis of $\hat{H}_{\perp}$. It is also of interest to note that the states

$$|\Omega_1\rangle \equiv |S\rangle_1 \otimes |T\rangle_2 \otimes \cdots \otimes |S(T)\rangle_n, \tag{E3}$$

$$|\Omega_2\rangle \equiv |T\rangle_1 \otimes |S\rangle_2 \otimes \cdots \otimes |T(S)\rangle_n \tag{E4}$$

are also zero-energy eigenstates of $\hat{H}_{\parallel}$ and so we will define these to be the "vacua" of the Hamiltonian $\hat{H}$.

From here, one can add "excitations" in the form of $|0\rangle$ or $|1\rangle$. This is because the Hamiltonian $\hat{H}_{\parallel}$ sends (cf. Eq. 2

in Ref. [78])

$$|0S\rangle \leftrightarrow |S0\rangle, \quad |0T\rangle \leftrightarrow |T0\rangle, \tag{E5a}$$

$$|1S\rangle \leftrightarrow |S1\rangle, \quad |1T\rangle \leftrightarrow |T1\rangle, \tag{E5b}$$

where $\leftrightarrow$ represents mapping under $\hat{H}_{\parallel}$ modulo multiplicative constants. Furthermore, $\hat{H}_{\parallel}|00\rangle = \hat{H}_{\parallel}|11\rangle = 0$ and so any fixed number of $|0\rangle$ *or* $|1\rangle$ particles on top of the vacuum can be mapped exactly to free fermions—each individual species experiences a nearest-neighbor-hopping Hamiltonian without scattering. The caveat here, and the reason why the entire Hilbert space is not equivalent to free fermions, is that the $|0\rangle$ particles and $|1\rangle$ particles can scatter off of each other. That is, $\hat{H}_{\parallel}$ maps (cf. Eq. 3 in Ref. [78])

$$|01\rangle + |10\rangle \leftrightarrow |TT\rangle - |SS\rangle. \tag{E6}$$

Hence, we can observe that for a given ground state and a given particle species, there are $\sum_{i=0}^{n} \binom{n}{i} = 2^n$ different states in the free-fermion subspace, giving overall a $(2^{n+2} - 4)$-dimensional Hilbert space. On the other hand, the total Hilbert-space dimension is 2^{2n}, so the free-fermion sector is exponentially large in n but still exponentially small compared to the full space.

We now demonstrate that the state

$$|\psi\rangle_{\text{ss}} = \bigotimes_{i=1}^{n}\left[\sqrt{1-v^2}|0\rangle_{A,i}|0\rangle_{B,i} + (-1)^{i}v|1\rangle_{A,i}|1\rangle_{B,i}\right] \tag{E7}$$

is an eigenstate of $\hat{H}_{\parallel} + \hat{H}_{\perp}$ and therefore a steady state of the Liouvillian

$$\hat{\mathcal{L}}\hat{\rho} = -i[\hat{H}_{\parallel} + \hat{H}_{\perp}, \hat{\rho}] + \hat{\mathcal{L}}_{\text{diss}}\hat{\rho}, \tag{E8}$$

with $\hat{\mathcal{L}}_{\text{diss}}$ as given in Eq. (35) in the main text. We have already noted that $\hat{H}_{\parallel}|\psi\rangle_{\text{ss}} = 0$, so it remains only to show that $\hat{H}_{\perp}|\psi\rangle_{\text{ss}} = nJ_z|\psi\rangle_{\text{ss}}$. By direct computation, we can observe that

$$\hat{H}_{\perp}|\psi\rangle_{\text{ss}} = \left[\sum_{i=1}^{n} J\left(\hat{\sigma}_{A,i}^{x}\hat{\sigma}_{B,i}^{x} + \hat{\sigma}_{A,i}^{y}\hat{\sigma}_{B,i}^{y}\right) + J_z\hat{\sigma}_{A,i}^{z}\hat{\sigma}_{B,i}^{z}\right]\bigotimes_{j=1}^{n}\left[\sqrt{1-v^2}|0\rangle_{A,j}|0\rangle_{B,j} + (-1)^{j}v|1\rangle_{A,j}|1\rangle_{B,j}\right]$$

$$= \left[\sum_{i=1}^{n} J_z\hat{\sigma}_{A,i}^{z}\hat{\sigma}_{B,i}^{z}\right]\bigotimes_{j=1}^{n}\left[\sqrt{1-v^2}|0\rangle_{A,j}|0\rangle_{B,j} + (-1)^{j}v|1\rangle_{A,j}|1\rangle_{B,j}\right]$$

$$= \left[\sum_{i=1}^{n} J_z\right]\bigotimes_{j=1}^{n}\left[\sqrt{1-v^2}|0\rangle_{A,j}|0\rangle_{B,j} + (-1)^{j}v|1\rangle_{A,j}|1\rangle_{B,j}\right] = nJ_z|\psi\rangle_{\text{ss}}, \tag{E9}$$

as desired.

APPENDIX F: DERIVATION OF LOCAL LINDBLAD MASTER EQUATIONS FROM SYSTEM-BATH COUPLING

Here, we will derive how one obtains a Lindblad-style master equation with jump operators respecting the locality constraint [cf. Eq. (6)] starting from a system-bath coupling of the form given in Eq. (8). We will follow the general procedure of taking first the Born-Markov and then rotating-wave approximations, as laid out in, e.g., Refs. [44,45]. We will not thoroughly justify each approximation, as this has already been explained in great detail elsewhere (for these details, we encourage the reader to consult Refs. [44,45]). We begin by assuming that we have a tripartite quantum system, with a Hilbert space $\mathcal{H} = \mathcal{H}_R \otimes \mathcal{H}_A \otimes \mathcal{H}_B$. Overall, these describe a reservoir ($\mathcal{H}_R$), which will be traced out to give the open-system dynamics, along with a bipartite system composed of $\mathcal{H}_{A,B}$. The full Hamiltonian can be written in the form

$$\hat{H} = \hat{H}_R + \hat{H}_S + \hat{H}_I, \tag{F1}$$

with $\hat{H}_R$ giving local dynamics of the reservoir, $\hat{H}_S$ local dynamics of the bipartite system, and $\hat{H}_I$ giving their (weak) interaction. We will assume that the local dynamics $\hat{H}_S$ can be further decomposed as $\hat{H}_S = \hat{H}_A + \hat{H}_B$, so that there is no explicit interaction between subsystems not mediated by the reservoir.

Now, let us define $\hat{\tilde{\chi}}(t)$ to be the density matrix for the entire system plus reservoir. It is governed by an equation of motion,

$$\partial_t \hat{\tilde{\chi}} = -i[\hat{H}, \hat{\tilde{\chi}}]. \tag{F2}$$

If we work in the interaction picture of the local dynamics, we can define $\hat{\mathcal{U}} = \exp\left(it\left(\hat{H}_R + \hat{H}_S\right)\right)$ so that $\hat{\chi}(t) = \hat{\mathcal{U}}\hat{\tilde{\chi}}(t)\hat{\mathcal{U}}^\dagger$ simply obeys

$$\partial_t \hat{\chi} = -i[\hat{H}_I(t), \hat{\chi}]. \tag{F3}$$

From here, we can formally integrate the equation of motion to find that

$$\hat{\chi}(t) = \hat{\chi}(0) - i\int_0^t [\hat{H}_I(s), \hat{\chi}(s)] \, ds. \tag{F4}$$

At this point, we can define the system density matrix $\hat{\rho}$ as the partial trace over the reservoir degrees of freedom: $\hat{\rho} = \mathrm{tr}_R \hat{\chi}$. This gives an equation of motion

$$\partial_t \hat{\rho} = -\int_0^t \mathrm{tr}_B[\hat{H}_I(t), [\hat{H}_I(s), \hat{\chi}(s)]] \, ds. \tag{F5}$$

To this point, the equation is exact. However, to make progress, we will make the Born-Markov approximation

that the full density matrix $\hat{\chi}(t) \approx \hat{\rho}(t) \otimes \hat{\rho}_R$ for all times: i.e. the reservoir is always approximately in the same state ρ_R, which we take to be static (diagonal in the eigenvectors of $\hat{H}_R$; e.g., a thermal state). Next, we will assume that the local time dynamics only depend on the state at the given time, i.e., there is no memory effect. This allows us to replace $\hat{\chi}(s) \rightarrow \hat{\chi}(t)$ in the integral, giving the new equation of motion:

$$\partial_t \hat{\rho} = -\int_0^t \mathrm{tr}_B[\hat{H}_I(t), [\hat{H}_I(t-s), \hat{\rho}(t) \otimes \hat{\rho}_R]] \, ds. \tag{F6}$$

The fact that we have replaced $\hat{\chi}(t)$ with $\hat{\chi}(s)$ tells us that the integration kernel should be tightly peaked around $|t - s| \sim 0$ and so we can extend the upper integration bound to infinity with very little error. This finally gives the time-local Redfield equation:

$$\partial_t \hat{\rho} = -\int_0^\infty \mathrm{tr}_B[\hat{H}_I(t), [\hat{H}_I(t-s), \hat{\rho}(t) \otimes \hat{\rho}_R]] \, ds. \tag{F7}$$

To get something in Lindblad form, we must now make the rotating-wave approximation. For this, it will be necessary to recall the exact form of the interaction Hamiltonian:

$$\hat{H}_I = \sum_{\mu=1}^M \hat{R}_{A,\mu} \otimes \hat{\tilde{A}}_\mu \otimes \mathbb{1} + \hat{R}_{B,\mu} \otimes \mathbb{1} \otimes \hat{\tilde{B}}_\mu + \text{H.c.}$$
$$= \sum_{j=1}^{4M} \hat{R}'_j \otimes \hat{S}'_j, \tag{F8}$$

$$\hat{R}'_j = \begin{cases} \frac{1}{\sqrt{2}}(\hat{R}_{A,j} + \hat{R}^\dagger_{A,j}), & 1 \leq j \leq M, \\ \frac{i}{\sqrt{2}}(\hat{R}_{A,j-M} - \hat{R}^\dagger_{A,j-M}), & M < j \leq 2M, \\ \frac{1}{\sqrt{2}}(\hat{R}_{B,j-2M} + \hat{R}^\dagger_{B,j-2M}), & 2M < j \leq 3M, \\ \frac{i}{\sqrt{2}}(\hat{R}_{B,j-3M} - \hat{R}^\dagger_{B,j-3M}), & 3M < j \leq 4M, \end{cases} \tag{F9}$$

$$\hat{S}'_j = \begin{cases} \frac{1}{2}(\hat{\tilde{A}}_j + \hat{\tilde{A}}^\dagger_j) \otimes \mathbb{1}, & 1 \leq j \leq M, \\ \frac{i}{2}(\hat{\tilde{A}}_{j-M} - \hat{\tilde{A}}^\dagger_{j-M}) \otimes \mathbb{1}, & M < j \leq 2M, \\ \frac{1}{2}\mathbb{1} \otimes (\hat{\tilde{B}}_{j-2M} + \hat{\tilde{A}}^\dagger_{j-2M}), & 2M < j \leq 3M, \\ \frac{i}{2}\mathbb{1}s \otimes (\hat{\tilde{B}}_{j-3M} - \hat{\tilde{A}}^\dagger_{j-3M}), & 3M < j \leq 4M, \end{cases} \tag{F10}$$

where we have defined $\hat{R}'_j$ and $\hat{S}'_j$ to be Hermitian operators that act on either the reservoir or the system, respectively. It will also be extremely important to observe that each system operator is local to either the A or B subsystem. Next, we will decompose the system operators $\hat{S}'_j$ into their

frequency components. If we define the operator $\hat{\Pi}_\epsilon$ as the projector onto the eigenspace of $\hat{H}_S$ with eigenvalue ϵ, then we can rewrite

$$\hat{S}'_j = \sum_\omega \hat{S}'_j(\omega), \tag{F11}$$

$$\hat{S}'_j(\omega) = \sum_{\epsilon - \epsilon' = \omega} \hat{\Pi}_{\epsilon'} \hat{S}'_j \hat{\Pi}_\epsilon. \tag{F12}$$

Using these operators, we can now expand the equation of motion as

$$\partial_t \hat{\rho} = \sum_{\omega, \omega', j, k} e^{i(\omega - \omega')t} C_{jk}(\omega)$$
$$\times \left[\hat{S}'_j(\omega) \hat{\rho} \hat{S}'_j(\omega')^\dagger - \hat{S}'_j(\omega')^\dagger \hat{S}'_j(\omega) \hat{\rho} \right] + \text{H.c.}, \tag{F13}$$

$$C_{jk}(\omega) = \int_0^\infty e^{i\omega s} \langle \hat{R}_j^\dagger(t) \hat{R}_k(s - t) \rangle \, ds$$
$$= \int_0^\infty e^{i\omega s} \langle \hat{R}_j^\dagger(s) \hat{R}_k(0) \rangle \, ds, \tag{F14}$$

where in the second line we have used the stationarity of $\hat{\rho}_R$. Finally, we make the secular approximation and neglect rapidly rotating terms. Thus, we finally arrive at

$$\partial_t \hat{\rho} = \sum_{\omega, j, k} C_{jk}(\omega) \left[\hat{S}'_j(\omega) \hat{\rho} \hat{S}'_k(\omega)^\dagger - \hat{S}'_k(\omega)^\dagger \hat{S}'_j(\omega) \hat{\rho} \right] + \text{H.c.} \tag{F15}$$

From here, we can define

$$\gamma_{jk}(\omega) = C_{jk}(\omega) + C_{kj}(\omega)^*, \tag{F16}$$

$$h_{jk}(\omega) = \frac{-i}{2} \left(C_{jk}(\omega) - C_{kj}(\omega)^* \right), \tag{F17}$$

$$\hat{H}_{LS} = \sum_{jk\omega} h_{jk}(\omega) \hat{S}'^\dagger_j(\omega) \hat{S}'_k(\omega). \tag{F18}$$

$\hat{H}_{LS}$ is the Lamb-shift Hamiltonian and γ_{jk} describes the dissipative part of the dynamics:

$$\partial_t \hat{\rho} = -i[\hat{H}_{LS}, \hat{\rho}] + \hat{\mathcal{L}}_{\text{diss}} \hat{\rho}, \tag{F19}$$

$$\hat{\mathcal{L}}_{\text{diss}} \hat{\rho} = \sum_{\omega, j, k} \gamma_{jk}(\omega) \left[\hat{S}'_j(\omega) \hat{\rho} \hat{S}'_k(\omega)^\dagger - \frac{1}{2} \left\{ \hat{S}'_k(\omega)^\dagger \hat{S}'_j(\omega), \hat{\rho} \right\} \right]. \tag{F20}$$

The matrix $\gamma_{jk}(\omega)$ is positive and so it can be unitarily diagonalized. Taking $U(\omega)$ to be a unitary matrix, we can rewrite

$$\gamma_{jk}(\omega) = \kappa_l(\omega) U^*_{lj}(\omega) U_{lk}(\omega). \tag{F21}$$

The dissipation can then be rewritten as

$$\hat{\mathcal{L}}_{\text{diss}} \hat{\rho} = \sum_{\omega, l} \mathcal{D}[\hat{L}_l(\omega)] \hat{\rho}, \tag{F22}$$

$$\hat{L}_l(\omega) = \sum_n U^*_{ln}(\omega) \hat{S}'_n(\omega). \tag{F23}$$

Recall that when we began, each operator $\hat{S}'_j$ was local to one of the two subsystems [cf. Eq. (F10)]. Moreover, because $\hat{H}_S = \hat{H}_A + \hat{H}_B$ contains no interactions between the subsystems, the projections into frequency space, $\hat{S}'_j(\omega)$, must also remain local to a single sublattice (i.e., the dynamics of two noninteracting subsystems cannot mix local operators together). Thus, each jump operator in Eq. (F23) is a sum of local operators, as we set out to prove. Moreover, we can observe that the Lamb-shift Hamiltonian in Eq. (F18) is quadratic in $\hat{S}'_j(\omega)$ and so after tracing out the reservoir there will generically be long-range Hamiltonian interactions between the two systems. Such a Lamb-shift Hamiltonian is generically constrained by the form of the dissipation (via Kramers-Kronig relations); however, we take it to be arbitrary since it does not affect any of the final results given in the main text.

APPENDIX G: NUMERICAL TECHNIQUES

In this appendix, we outline the numerical techniques used to generate the random models as presented in, e.g., Fig. 2. The algorithm used can be summarized into the following steps:

(1) *Generate the steady state.* The first step is to generate the steady state. We pick a value of the entanglement $\delta \mathcal{E}_2$ and run an optimization algorithm to find a set of Schmidt coefficients such that the normalization is fixed to unity and the Renyi-2 entropy is fixed, beginning from a set of random values.

(2) *Generate jump operators.* Next, we generate a random $N \times N$ matrix sampled from the random complex Ginibre ensemble, which becomes the A matrix. [If we wish to use a different ensemble, we follow the prescription in Eq. (B3).] We then use this along with the Schmidt coefficients from step (1) to generate B uniquely using Eq. (24). We repeat this M times to generate M jump operators.

(3) *Generate Hamiltonian.* If we are simulating directional dynamics, we generate a Hamiltonian as prescribed in Eq. (D8). Otherwise, we proceed to the next step.

(4) *Find dissipative gap*. Given the matrices A and B generated in step (2) and the Hamiltonian in step (3) (if present), we use the QuTip [80] software package to generate a Liouvillian superoperator. We extract its eigenvalues, from which we can find the dissipative gap.

These steps generate a single data point for a fixed N, M, $\delta\mathcal{E}_2$, and distribution. Each plot samples from 20 different values of $\delta\mathcal{E}_2$ and samples different random models from each value to get good convergence of the average and standard deviation, usually about 100 samples for each.

To be even more explicit, we will now go through a specific example of generating such a system for $N = 2$ and $M = 1$. First we perform step (1). Note that because we have two constraints (normalization and entanglement) and two Schmidt coefficients, they are exactly specified. We can write the matrix Ψ as

$$\Psi = \begin{pmatrix} \frac{1}{2} - p & 0 \\ 0 & \frac{1}{2} + p \end{pmatrix}, \tag{G1}$$

$$p = \sqrt{\frac{\delta\mathcal{E}_2}{2}}. \tag{G2}$$

Next, we do step (2) and generate a random matrix A, which we will leave unspecified as

$$A = \begin{pmatrix} a_{11} & a_{12} \\ a_{21} & a_{22} \end{pmatrix}. \tag{G3}$$

This allows us to uniquely specify a matrix B as

$$B = -\Psi A^T \Psi^{-1} = \begin{pmatrix} -a_{11} & \xi a_{21} \\ \xi^{-1} a_{12} & -a_{22} \end{pmatrix}, \tag{G4}$$

$$\xi = \frac{2p - 1}{2p + 1}. \tag{G5}$$

Since we are not using directional dynamics, we can now proceed directly to step (4) and generate a Liouvillian superoperator. To do this, we first need to find the jump operator $L = A \otimes \mathbb{1} + \mathbb{1} \otimes B$, which can be written as

$$L = \begin{pmatrix} 0 & \xi a_{21} & a_{12} & 0 \\ \xi^{-1} a_{12} & a_{11} - a_{22} & 0 & a_{12} \\ a_{21} & 0 & a_{22} - a_{11} & \xi a_{21} \\ 0 & a_{21} & \xi^{-1} a_{12} & 0 \end{pmatrix}. \tag{G6}$$

From here, it is simple to use this matrix to generate a Lindbladian and find its spectrum.

[1] M. B. Hastings, An area law for one-dimensional quantum systems, J. Stat. Mech.: Theory Exp. **2007**, P08024 (2007).

[2] T. Kuwahara and K. Saito, Area law of noncritical ground states in 1D long-range interacting systems, Nat. Commun. **11**, 4478 (2020).

[3] Z.-X. Gong, M. Foss-Feig, F. G. S. L. Brandão, and A. V. Gorshkov, Entanglement area laws for long-range interacting systems, Phys. Rev. Lett. **119**, 050501 (2017).

[4] L. Masanes, Area law for the entropy of low-energy states, Phys. Rev. A **80**, 052104 (2009).

[5] A. Anshu, I. Arad, and D. Gosset, in *Proceedings of the 54th Annual ACM SIGACT Symposium on Theory of Computing*, STOC 2022 (Association for Computing Machinery, New York, 2022), p. 12.

[6] F. G. S. L. Brandão and M. Cramer, Entanglement area law from specific heat capacity, Phys. Rev. B **92**, 115134 (2015).

[7] J. Cho, Sufficient condition for entanglement area laws in thermodynamically gapped spin systems, Phys. Rev. Lett. **113**, 197204 (2014).

[8] S. Michalakis and J. P. Zwolak, Stability of frustration-free Hamiltonians, Commun. Math. Phys. **322**, 277 (2013).

[9] M. M. Wolf, F. Verstraete, M. B. Hastings, and J. I. Cirac, Area laws in quantum systems: Mutual information and correlations, Phys. Rev. Lett. **100**, 070502 (2008).

[10] N. de Beaudrap, M. Ohliger, T. J. Osborne, and J. Eisert, Solving frustration-free spin systems, Phys. Rev. Lett. **105**, 060504 (2010).

[11] J. Eisert, M. Cramer, and M. B. Plenio, Colloquium: Area laws for the entanglement entropy, Rev. Mod. Phys. **82**, 277 (2010).

[12] G. Lindblad, On the generators of quantum dynamical semigroups, Commun. Math. Phys. **48**, 119 (1976).

[13] V. Gorini, A. Kossakowski, and E. C. G. Sudarshan, Completely positive dynamical semigroups of n-level systems, J. Math. Phys. **17**, 821 (1976).

[14] M. J. Kastoryano and J. Eisert, Rapid mixing implies exponential decay of correlations, J. Math. Phys. **54**, 102201 (2013).

[15] F. G. S. L. Brandão, T. S. Cubitt, A. Lucia, S. Michalakis, and D. Perez-Garcia, Area law for fixed points of rapidly mixing dissipative quantum systems, J. Math. Phys. **56**, 102202 (2015).

[16] D. Poulin, Lieb-Robinson bound and locality for general Markovian quantum dynamics, Phys. Rev. Lett. **104**, 190401 (2010).

[17] J. F. Poyatos, J. I. Cirac, and P. Zoller, Quantum reservoir engineering with laser cooled trapped ions, Phys. Rev. Lett. **77**, 4728 (1996).

[18] M. B. Plenio and S. F. Huelga, Entangled light from white noise, Phys. Rev. Lett. **88**, 197901 (2002).

[19] B. Kraus and J. I. Cirac, Discrete entanglement distribution with squeezed light, Phys. Rev. Lett. **92**, 013602 (2004).

[20] S. G. Schirmer and X. Wang, Stabilizing open quantum systems by Markovian reservoir engineering, Phys. Rev. A **81**, 062306 (2010).

[21] K. Stannigel, P. Rabl, and P. Zoller, Driven-dissipative preparation of entangled states in cascaded quantum-optical networks, New J. Phys. **14**, 063014 (2012).

[22] S. Zippilli, M. Paternostro, G. Adesso, and F. Illuminati, Entanglement replication in driven dissipative many-body systems, Phys. Rev. Lett. **110**, 040503 (2013).

[23] F. Motzoi, E. Halperin, X. Wang, K. B. Whaley, and S. Schirmer, Backaction-driven, robust, steady-state long-distance qubit entanglement over lossy channels, Phys. Rev. A **94**, 032313 (2016).

[24] S. Ma, M. J. Woolley, I. R. Petersen, and N. Yamamoto, Pure Gaussian states from quantum harmonic oscillator chains with a single local dissipative process, J. Phys. A: Math. Theor. **50**, 135301 (2017).

[25] R. Ma, B. Saxberg, C. Owens, N. Leung, Y. Lu, J. Simon, and D. I. Schuster, A dissipatively stabilized Mott insulator of photons, Nature **566**, 51 (2019).

[26] E. Doucet, F. Reiter, L. Ranzani, and A. Kamal, High fidelity dissipation engineering using parametric interactions, Phys. Rev. Res. **2**, 023370 (2020).

[27] S. Zippilli and D. Vitali, Dissipative engineering of Gaussian entangled states in harmonic lattices with a single-site squeezed reservoir, Phys. Rev. Lett. **126**, 020402 (2021).

[28] J. Agustí, Y. Minoguchi, J. M. Fink, and P. Rabl, Long-distance distribution of qubit-qubit entanglement using Gaussian-correlated photonic beams, Phys. Rev. A **105**, 062454 (2022).

[29] L. C. G. Govia, A. Lingenfelter, and A. A. Clerk, Stabilizing two-qubit entanglement by mimicking a squeezed environment, Phys. Rev. Res. **4**, 023010 (2022).

[30] T. Brown, E. Doucet, D. Ristè, G. Ribeill, K. Cicak, J. Aumentado, R. Simmonds, L. Govia, A. Kamal, and L. Ranzani, Trade off-free entanglement stabilization in a superconducting qutrit-qubit system, Nat. Commun. **13**, 3994 (2022).

[31] J. Angeletti, S. Zippilli, and D. Vitali, Dissipative stabilization of entangled qubit pairs in quantum arrays with a single localized dissipative channel, Quantum Sci. Technol. **8**, 035020 (2023).

[32] A. Lingenfelter, M. Yao, A. Pocklington, Y.-X. Wang, A. Irfan, W. Pfaff, and A. A. Clerk, Exact results for a boundary-driven double spin chain and resource-efficient remote entanglement stabilization, arXiv:2307.09482.

[33] S. Diehl, A. Micheli, A. Kantian, B. Kraus, H. P. Büchler, and P. Zoller, Quantum states and phases in driven open quantum systems with cold atoms, Nat. Phys. **4**, 878 (2008).

[34] B. Kraus, H. P. Büchler, S. Diehl, A. Kantian, A. Micheli, and P. Zoller, Preparation of entangled states by quantum Markov processes, Phys. Rev. A **78**, 042307 (2008).

[35] S. Diehl, E. Rico, M. A. Baranov, and P. Zoller, Topology by dissipation in atomic quantum wires, Nat. Phys. **7**, 971 (2011).

[36] A. Pocklington, Y.-X. Wang, Y. Yanay, and A. A. Clerk, Stabilizing volume-law entangled states of fermions and qubits using local dissipation, Phys. Rev. B **105**, L140301 (2022).

[37] S. Zippilli, J. Li, and D. Vitali, Steady-state nested entanglement structures in harmonic chains with single-site squeezing manipulation, Phys. Rev. A **92**, 032319 (2015).

[38] J. Guo, O. Hart, C.-F. Chen, A. J. Friedman, and A. Lucas, Designing open quantum systems with known steady states: Davies generators and beyond, arXiv:2404.14538.

[39] C.-F. Chen, M. J. Kastoryano, F. G. S. L. Brandão, and A. Gilyén, Quantum thermal state preparation, arXiv:2303.18224.

[40] Z. Ding, B. Li, and L. Lin, Efficient quantum Gibbs samplers with Kubo-Martin-Schwinger detailed balance condition, arXiv:2404.05998.

[41] S.-K. Sun and S. Chen, Emergence of Gibbs ensemble as the unique steady state in open quantum systems, arXiv:2406.18041.

[42] M. Mamaev, M. Koppenhöfer, A. Pocklington, and A. A. Clerk, Non-Gaussian generalized two-mode squeezing: Applications to two-ensemble spin squeezing and beyond, arXiv:2407.00721.

[43] Observe that because the (e.g., Bures) metric is contractive under completely positive trace-preserving maps, then by the contraction-mapping theorem, the Lindblad generator acting on a finite-dimensional Hilbert space must have a zero eigenvalue. Hence, we define this zero eigenvalue to be λ_0 and arrange all remaining eigenvalues according to their real parts.

[44] H.-P. Breuer and F. Petruccione, *The Theory of Open Quantum Systems* (Oxford University Press, New York, 2002).

[45] C. Gardiner and P. Zoller, *Quantum Noise: A Handbook of Markovian and non-Markovian Quantum Stochastic Methods with Applications to Quantum Optics*, Springer Series in Synergetics (Springer-Verlag, Berlin, 2004).

[46] H. M. Wiseman and G. J. Milburn, Quantum theory of optical feedback via homodyne detection, Phys. Rev. Lett. **70**, 548 (1993).

[47] H. M. Wiseman and G. J. Milburn, Squeezing via feedback, Phys. Rev. A **49**, 1350 (1994).

[48] A. Metelmann and A. A. Clerk, Nonreciprocal quantum interactions and devices via autonomous feedforward, Phys. Rev. A **95**, 013837 (2017).

[49] H. M. Wiseman and G. J. Milburn, *Quantum Measurement and Control* (Cambridge University Press, Cambridge, UK, 2009).

[50] C. M. Caves and B. L. Schumaker, New formalism for two-photon quantum optics. I. Quadrature phases and squeezed states, Phys. Rev. A **31**, 3068 (1985).

[51] C. C. Gerry, Dynamics of SU(1,1) coherent states, Phys. Rev. A **31**, 2721 (1985).

[52] A. Pocklington, Y.-X. Wang, and A. A. Clerk, Dissipative pairing interactions: Quantum instabilities, topological light, and volume-law entanglement, Phys. Rev. Lett. **130**, 123602 (2023).

[53] B. Buča and T. Prosen, A note on symmetry reductions of the Lindblad equation: Transport in constrained open spin chains, New J. Phys. **14**, 073007 (2012).

[54] K. Temme, M. J. Kastoryano, M. B. Ruskai, M. M. Wolf, and F. Verstraete, The χ^2-divergence and mixing times of quantum Markov processes, J. Math. Phys. **51**, 122201 (2010).

[55] M. A. Nielsen and I. L. Chuang, Quantum computation and quantum information, Phys. Today **54**, 60 (2001).

[56] F. Fagnola and V. Umanita, Generators of detailed balance quantum Markov semigroups, Infin. Dimens. Anal. Quantum Probab. Relat. Top. **10**, 335 (2007).

[57] F. Fagnola and V. Umanità, Generators of KMS symmetric Markov semigroups on $\mathcal{B}(h)$ symmetry and quantum detailed balance, Commun. Math. Phys. **298**, 523 (2010).

[58] D. Roberts, A. Lingenfelter, and A. Clerk, Hidden time-reversal symmetry, quantum detailed balance and exact solutions of driven-dissipative quantum systems, PRX Quantum **2**, 020336 (2021).

[59] D. Roberts and A. A. Clerk, Driven-dissipative quantum Kerr resonators: New exact solutions, photon blockade and quantum bistability, Phys. Rev. X **10**, 021022 (2020).

[60] M. Tsang, Quantum reversal: A general theory of coherent quantum absorbers, arXiv:2402.02502.

[61] W. Cottrell, B. Freivogel, D. M. Hofman, and S. F. Lokhande, How to build the thermofield double state, J. High Energy Phys. **2019**, 58 (2019).

[62] J. c. v. Bensa and M. Žnidarič, Fastest local entanglement scrambler, multistage thermalization, and a non-Hermitian phantom, Phys. Rev. X **11**, 031019 (2021).

[63] J. c. v. Bensa and M. Žnidarič, Two-step phantom relaxation of out-of-time-ordered correlations in random circuits, Phys. Rev. Res. **4**, 013228 (2022).

[64] G. Lee, A. McDonald, and A. Clerk, Anomalously large relaxation times in dissipative lattice models beyond the non-Hermitian skin effect, Phys. Rev. B **108**, 064311 (2023).

[65] S. Yao and Z. Wang, Edge states and topological invariants of non-Hermitian systems, Phys. Rev. Lett. **121**, 086803 (2018).

[66] T. E. Lee, Anomalous edge state in a non-Hermitian lattice, Phys. Rev. Lett. **116**, 133903 (2016).

[67] F. K. Kunst, E. Edvardsson, J. C. Budich, and E. J. Bergholtz, Biorthogonal bulk-boundary correspondence in non-Hermitian systems, Phys. Rev. Lett. **121**, 026808 (2018).

[68] A. McDonald, T. Pereg-Barnea, and A. A. Clerk, Phase-dependent chiral transport and effective non-Hermitian dynamics in a bosonic kitaev-majorana chain, Phys. Rev. X **8**, 041031 (2018).

[69] K. Kawabata, K. Shiozaki, M. Ueda, and M. Sato, Symmetry and topology in non-Hermitian physics, Phys. Rev. X **9**, 041015 (2019).

[70] V. M. Martinez Alvarez, J. E. Barrios Vargas, and L. E. F. Foa Torres, Non-Hermitian robust edge states in one dimension: Anomalous localization and eigenspace condensation at exceptional points, Phys. Rev. B **97**, 121401(R) (2018).

[71] T. Haga, M. Nakagawa, R. Hamazaki, and M. Ueda, Liouvillian skin effect: Slowing down of relaxation processes without gap closing, Phys. Rev. Lett. **127**, 070402 (2021).

[72] S. Denisov, T. Laptyeva, W. Tarnowski, D. Chruściński, and K. Życzkowski, Universal spectra of random Lindblad operators, Phys. Rev. Lett. **123**, 140403 (2019).

[73] F. Reiter and A. S. Sørensen, Effective operator formalism for open quantum systems, Phys. Rev. A **85**, 032111 (2012).

[74] H. J. Carmichael, Quantum trajectory theory for cascaded open systems, Phys. Rev. Lett. **70**, 2273 (1993).

[75] C. W. Gardiner, Driving a quantum system with the output field from another driven quantum system, Phys. Rev. Lett. **70**, 2269 (1993).

[76] A. Metelmann and A. A. Clerk, Nonreciprocal photon transmission and amplification via reservoir engineering, Phys. Rev. X **5**, 021025 (2015).

[77] W. Tarnowski, D. Chruściński, S. Denisov, and K. Życzkowski, Random Lindblad operators obeying detailed balance, Open Syst. Inf. Dyn. **30**, 2350007 (2023).

[78] M. Žnidarič, Coexistence of diffusive and ballistic transport in a simple spin ladder, Phys. Rev. Lett. **110**, 070602 (2013).

[79] A. del Campo, I. L. Egusquiza, M. B. Plenio, and S. F. Huelga, Quantum speed limits in open system dynamics, Phys. Rev. Lett. **110**, 050403 (2013).

[80] J. Johansson, P. Nation, and F. Nori, Qutip: An open-source PYTHON framework for the dynamics of open quantum systems, Comput. Phys. Commun. **183**, 1760 (2012).